Michael C. Breadmore[1]
Ria Marni Tubaon[1]
Aliaa I. Shallan[1]
Sui Ching Phung[1]
Aemi S. Abdul Keyon[1,2]
Daniel Gstoettenmayr[1]
Pornpan Prapatpong[3]
Ala A. Alhusban[4]
Leila Ranjbar[1]
Hong Heng See[1,5]
Mohamed Dawod[6,7]
Joselito P. Quirino[1]

[1]School of Physical Science, Australian Centre of Research on Separation Science, University of Tasmania, Hobart, Tasmania, Australia*

Received September 1, 2014
Revised September 25, 2014
Accepted September 25, 2014

Review

Recent advances in enhancing the sensitivity of electrophoresis and electrochromatography in capillaries and microchips (2012–2014)

One of the most cited limitations of capillary (and microchip) electrophoresis is the poor sensitivity. This review continues to update this series of biannual reviews, first published in *Electrophoresis* in 2007, on developments in the field of on-line/in-line concentration methods, covering the period July 2012–July 2014. It includes developments in the field of stacking, covering all methods from field-amplified sample stacking and large-volume sample stacking, through to ITP, dynamic pH junction, and sweeping. Attention is also given to on-line or in-line extraction methods that have been used for electrophoresis.

Keywords:
Extraction / Focusing / Preconcentration / Stacking / Sweeping
DOI 10.1002/elps.201400420

1 Introduction

Poor sensitivity is one of the often cited limitations of electrophoresis, particularly in comparison to LC, with concentration detection limits typically two to three orders of magnitude worse [1]. To overcome this problem, many different and unique approaches have been developed. Over the last 2 years since the last update, there has again been considerable interest in this topic, as shown in Fig. 1, which shows the number of manuscripts published that discuss "stacking." Interest in this topic appears to have leveled at approximately 150 papers per year since 2006. While there are papers describing the implementation of these methods in microchips, the reality is that the field is still dominated by the capillary format.

The aim of this review is to continue to highlight developments within the field of on-line concentration for electrophoresis, in both capillaries and microchips, and follows previous reviews on the topic published in 2007 [2], 2009 [3], 2011 [4], and 2013 [2] and compliments other reviews published over this time [3–18]. This review does not aim to be comprehensive, but to identify works that are of significance to the field that have been published between July 2012 and June 2014. The same classifications that have been used previously will be kept here and the material has been assembled in the same categories: concentration approaches based on electrophoretic phenomena will be broadly discussed as "stacking," while those involving partitioning onto or into a distinct phase will be considered as "extraction." This review will discuss approaches within the context of these two broad areas with the critical requirement that they are integrated in some manner, preferably *in-line* (performed within the capillary) or *on-line* (performed in a completely integrated and automated manner). For those who would like a more practical focus, Breadmore and Sänger-Van De Griend propose a decision tree to help select the right method for the right application [19].

2 Stacking

"Stacking" is a very widely used term within the electrophoretic community, and we will continue to use it in this review as a generic term to group approaches for

Correspondence: Dr. Michael Breadmore, School of Chemistry, Australian Centre for Research on Separation Science, University of Tasmania, GPO Box 252-75, Hobart, Tasmania 7001, Australia
Fax: +61-3-6226-2858
E-mail: mcb@utas.edu.au

Abbreviations: AFMC, analyte focusing by micelle collapse; **CF**, counterflow; **4-CP**, 4-chlorophenol; **2,4-DCP**, 2,4-dichlorophenol; **dzITP**, depletion zone ITP; **EDL**, electric double layer; **EKI**, electrokinetic injection; **EKS**, electrokinetic supercharging; **EME**, electromembrane extraction; **FASI**, field-amplified sample injection; **FASS**, field-amplified sample stacking; **FESI**, field enhance sample injection; **GEITP**, gradient elution ITP; **ICP**, ion concentration polarization; **LE**, leading electrolyte; **LLE**, liquid–liquid extraction; **LVSS**, large-volume sample stacking; **MSS**, micelle to solvent stacking; **NMI**, nano/microchannel interface; **PDADMAC**, poly(diallyldimethylammonium chloride); **pITP**, pseudo-ITP; **SDME**, single-drop microextraction; **SEF**, sensitivity enhancement factor; **SLM**, supported liquid membrane; **STDC**, sodium taurodeoxycholate; **2,4,6-TCP**, 2,4,6-trichlorophenol; **TE**, terminating/trailing electrolyte; **tITP**, transient ITP

*For other affiliations, please see Addendum.

Colour Online: See the article online to view Figs. 1, 3–7, 9, 11 and 14 in colour.

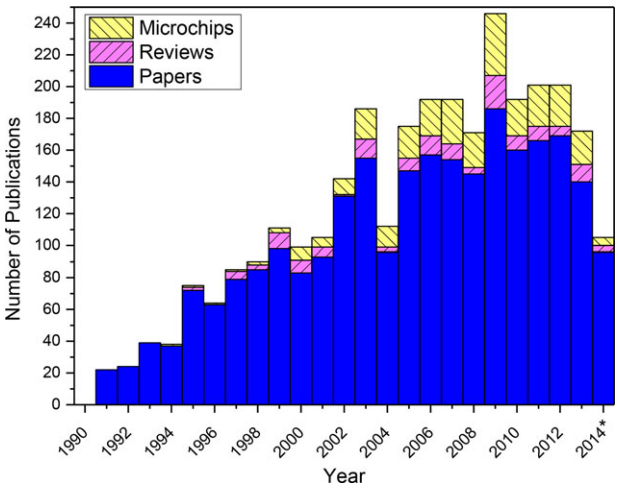

Figure 1. Prevalence of on-line concentration for electrophoresis as obtained from ISI Web of Science using "stacking or sweeping" and "electrophor*" in the topic. Number of papers for 2014 is up until 30th June.

concentration that rely on changes in electrophoretic velocity. This encompasses preconcentration induced via changes in field strength as well as changes in electrophoretic velocity achieved through other means (such as sweeping). In all cases, the key requirement is that there is an electrophoretic component in the preconcentration mechanism and that the analytes concentrate on a boundary through a change in velocity.

2.1 Field-strength induced changes in velocity

2.1.1 Field-amplified sample stacking (FASS) and field-amplified sample injection (FASI)

FASS, also known as normal stacking mode, is the easiest sample stacking technique to perform as it only requires the sample to have a conductivity at most one-tenth of the conductivity of the BGE. Due to the difference in resistivity of the two different solutions, the electric field strength in the sample zone is higher than that in the BGE zone. Since ion velocity is proportional to the electric field strength, ions move quickly through the sample and slow down once they enter the BGE zone, in other words, they "stack" into a narrow zone at the interface. The sensitivity enhancement is determined by the ratio of velocities in the sample zone and BGE zone. The sensitivity enhancement factor (SEF) is usually around 10–20 times when compared to hydrodynamic injection of a sample with an equivalent conductivity to that of the BGE. There are two major drawbacks to this approach. First, that the sample should have a lower conductivity than that of the BGE, thus FASS is limited to samples with a low-conductivity matrix, or dilution of the sample is required. The other limitation of FASS is that the maximum length of the hydrodynamically injected sample plug is limited to about 3–5% of the capillary volume. The mismatch of the local electroosmotic velocities in the BGE zone and sample zone will cause band broadening if a longer sample zone is injected. FASS has been employed in many routine applications and has become the most popular approach for sensitivity enhancement, despite its limitations.

Dziomba et al. [20] developed a novel FASS method in which they repetitively injected four times and then performed a CZE separation. Each injection step for the cationic compounds consisted of a hydrodynamic injection at 0.6 psi for 53 s followed by steps of sample matrix removal through the simultaneous application of a counterpressure and voltage (–1 psi, 2 kV, 0.65 min) to retain the focused analytes in the capillary. They achieved an SEF for six cationic drugs of around 1.46–2.66 compared to FASS, and an SEF of 12–35 compared to a standard hydrodynamic injection at 0.5 psi for 5 s. With this approach, the limited sample plug length of 3–5% of the capillary volume could be effectively extended to 27%, although the modest gains do not suggest that this is an efficient process.

Single-step CE in a PMMA chip employing FASS was presented by Ono et al. [21]. The presented system allows introduction of sample and separation solution, FASS of the sample solution, and separation within 2 min, without the use of additional equipment. Uniquely, the surface tension (capillary forces) was used to introduce and constrain the separation solution and sample. Figure 2A shows that the liquid movement stops when the microchannel suddenly expands (termed capillary stop valve). This principle in combination with air vents (Fig. 2B) was used to achieve a defined sample plug to provide a simple and defined method of introducing sample hydrodynamically into a microchip for FASS. When using fluorescein in a tenfold diluted BGE, a threefold improvement in signal enhancement could be achieved compared to non-FASS conditions where the sample was diluted in the BGE.

In FASI (also reported in some publication as field enhance sample injection, FESI), the sample is introduced by electrokinetic injection (EKI) in contrast to FASS where it is introduced hydrodynamically. When performing EKI, the sample will be injected by the EOF as well as by its own electrophoretic movement, and thus the magnitude and direction of the EOF is very important. There are four major disadvantages to FASI. The first two are the same as for FASS, namely it is limited to samples with a conductivity at least ten times lower than the BGE and that that the sample matrix volume that can be introduced is limited to 3–5% of the capillary volume. The third disadvantage of FESI is that sample ions have different mobilities and are therefore injected to a different extent. This results in more of the higher mobility ions being injected. The final disadvantage is that because of the way injection is performed, the number of analyte ions entering the capillary significantly depends on the conductivity of the matrix and therefore it is susceptible to any samples where the matrix level can change. Despite these disadvantages, FESI can give up to a 1000-fold increase in sensitivity. Injection of a short water-plug prior to sample injection can enhance the repeatability. Since this approach prevents analytes from being lost from the inlet, it can also enhance the sensitivity [22].

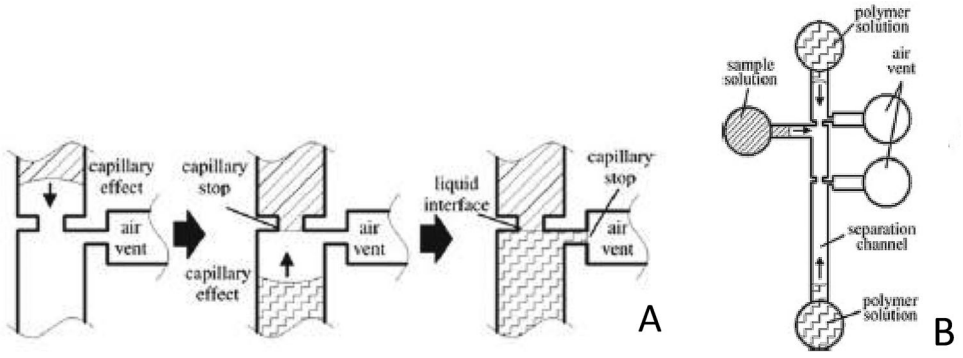

Figure 2. Schematic of the generation of a liquid interface using capillary stop valves and air vents (A) and schematic of the single-step CE setup (B) for controlled hydrodynamic injection of a sample in a microchip. Reproduced from [21] with permission.

Since the application of FESI is fairly straightforward, it can be combined with different detection methods such as inductively coupled plasma MS [23], electrochemiluminescence [24, 25], UV [26–28], quadrupole, IT, and TOF-MS [29], amperometric [30], and laser-induced fluorescence [31]. It can also be combined with different CE techniques such as open-tubular CEC [32] and chiral EKC [33]. Further it can be used in combination with off-line preconcentration methods such as dispersive liquid–liquid microextraction [34], dispersive liquid–liquid microextraction based on solidification of floating organic drop [35], ultrasound-assisted emulsification miocroextraction [36], and high-density solvent-based solvent de-emulsification dispersive liquid–liquid microextraction [37]. In fact, because of the clean and well-defined matrix that is obtained with these off-line methods, FASI is perfectly compatible with these and can provide excellent analytical results.

In an interesting twist on the use of FASI, Quirino used this approach for clean-up or purification of charged species from small sample volumes. FASI was repeatedly used to inject cationic small molecules from a 100 μL sample volume, with the sample then analyzed for anionic and neutral components. The results showed significant removal of interfering species without any compromise on the separation of the remaining compounds [38].

2.1.2. Large-volume sample stacking (LVSS)

LVSS was developed to allow the injection of sample volumes larger than can be achieved with FASS, and can be used to inject up to the entire capillary with sample, with both FASS and FASI. The key requirement for this approach to be successful is to slowly push the sample matrix out of the capillary inlet while the analytes are stacked at the sample/BGE interface. It is very important to stop the analytes exiting the inlet of the capillary before the separation begins. There are two ways to do this. The first is switch the polarity just before the stacked zone exits the capillary, and is typically done when the current reaches 90–95% of the BGE current. This approach was recently employed for the analysis of plant hormones [39], salidroside, caffeic acid, and gallic acid in leaf [40]; secobarbital, amobarbital, barbital, and phenobarbital in cosmetic products [41]; flavonoids [42], perfluorooctanoic acid, and perfluorooctanesulfonic acid in river water [43]; degradation products of alkyl alkylphosphonic acids in chemical warfare agent [44]; cephalosporins residue in environment water [45]; androgenic steroids [46] drugs in urine [47]; antiepileptic drug in serum [48]; and metformine in human urine and serum [49].

In a recent study, Qi et al. [50] used LVSS method with off-line SPE using molecular imprinted magnetic nanoparticles for the extraction of 4-chlorophenol (4-CP), 2,4-dichlorophenol (2,4-DCP), and 2,4,6-trichlorophenol (2,4,6-TCP) in environment water. The overall enhancement in sensitivity was 781, 3276, and 8916 for 4-CP, 2,4-DCP, and 2,4,6-TCP, respectively, with the SPE extraction combined with LVSS two-step sample preconcentration compared with the normal hydrodynamic injection (10 cm for 3s). As the signal enhancements of the analytes were contributed to the SPE extraction and LVSS, 28-, 62-, and 92-fold for 4-CP, 2,4-DCP, and 2,4,6-TCP come from SPE pretreatment. Importantly, the SPE helps to remove the variable composition of water matrices making the combined procedure suitable for the analysis of chlorophenols at low concentration levels.

The second way to control matrix removal with LVSS is with an EOF pump (called LVSEP) whereby the sample matrix is removed through the capillary by EOF. The key to the success of this approach is to ensure that there is a different EOF between the sample and BGE such that as the sample is removed, the net flow through the capillary changes. When only a small amount of matrix remains, then electrophoresis occurs and the components separate by conventional means. The advantage of this approach is that it is controlled by the chemistry, not by physically switching the polarity based on time (there is no instrument developed that will let the polarity be switched on a current level). The disadvantage is that it relies on accurate and repeatable control of the EOF.

Kawai et al. [51] obtained some impressive enhancements by combining LVSEP and pressure-assisted EKI. Pressure is applied to the inlet during EKI to prolong the time for removal of sample matrix and EKI of the sample. After a predetermined time, the voltage is stopped and the inlet changes to BGE for separation. The sensitivity of glucose oligomer was enhanced more than 8600-fold, while for the model

compound fluorescein it was over 110 000-fold at an EKI time for 15 min.

Tůma et al. [52] reported the monitoring of γ-aminobutyric acid, glycine, and glutamate for in vivo test in microdialysates of periaqueductal gray matter using LVSEP with a C^4D detector. The LODs were around 10 nM, which is similar to those obtained using LIF after derivatization. Shen et al. used LVSEP with off-line SPE for trace detection of thiols in seawater [53]. Tween 20 capped gold nanoparticles (Tween 20-AuNPs) were used for extraction with the Tween 20 reducing nonspecific adsorption as well as enhancing the dispersion of the particles sea water. Extraction from 10 mL of solution was obtained, with the extracted thiols released and o-phthaldialdehyde derivatized for LIF detection. Under the optimum condition, the LODs for five peptides were down to 0.1–6 pM, with the LVSEP allowing the injection volume to be increased from 10 to 60 nL. The overall SEF was greater than 20 000, and the authors suggest that this method has the lowest LOD for glutathione, γ-glutamylcysteine, and phytochelatin analogs reported.

LVSEP was recently used for a range of applications including parabens in cosmetics [54], selenomethionine enantiomers in selenized yeast after off-line SPE [55], glucose ladder, glycoprotein-derived oligosaccharides in plant lectin [56, 57]; benzylamine and 1-naphthylethylamine, chlorpheniramine, brompheniramine, and basic proteins (cytochrome c, ribonuclease A, lysozyme, and alpha-chymotrypsinogen A) [58]; racemic warfarin and ibuprofen for chiral analysis [59]; ima-amine, *N*-desmethyl matinib mesylate, and related compounds in capsule drugs [60]; isbenzylisoquinoline alkaloids [61]; kynurenine and tryptophan in human plasma used for biomarkers for immune systems [62]; and sulfonylurea herbicides in cereals [63].

2.1.3 Isotachophoretic stacking

Among all electrophoretic preconcentration methods in CE, ITP is well known to be a powerful and robust preconcentration method capable of concentrating trace of component in a high concentration of matrix ions. In ITP stacking, the sample is placed between the leading electrolyte (LE) and terminating/trailing electrolyte (TE). The difference in mobility between the LE (higher mobility) and TE (lower mobility) creates a nonuniform electric field upon application of voltage. As a result, samples ions with a mobility between the mobility of the leading and terminating ions stack in front of TE but behind of LE in a descending order based on their mobilities. The length of each zone depends on the concentration of each ion and the initial concentration of LE ions defined by Kohlrausch regulating function. Two types of ITP modes can be used, which are the "plateau-mode" and "peak mode" ITP. Plateau mode ITP occurs when the analyte is present in large amount allowing the formation of separate contiguous plateau like zones with locally uniform concentration [2, 64, 65]. Peak mode ITP occurs when the analyte present is an amount that is unable to reach their steady-state concentration, thus unable to form a contiguous zone, and is therefore focused as a sharp peak between two zones [66]. Peak mode has always occurred, but has only recently been defined, and is actually the mode required when coupling with other modes of electrophoresis, that is when using it as a stacking approach.

Over the past few years, Santiago's group has been exceptionally active in the use of peak mode ITP. Since the last review, they extend from the purification of nucleic acids from whole blood to rapid in-line hybridization of RNA and DNA using molecular probes. In this area, Bercovici et al. [67] studied the physicochemical process of preconcentration, mixing, and chemical reaction kinetics by comparing numerical and experimental results. When 20 nM of target DNA was used, a 960-fold acceleration of the hybridization rate was obtained with ITP compared to a standard incubation, which increased to 14 000-fold when the target concentration was 500 pM. While impressive, there is still a background signal from unhbyridized nucleotide probe, which migrates with the hybridized DNA. Recent focus has been on ways to remove this, through hydrogels that contain the complimentary nucleotide to remove unhybridized probe [68], bidirectional ITP to initiate the transition from ITP to ZE [69], and the use a two-stage separation in which an ionic spacer is introduced during the second stage [70]. Garcia-Schwarz et al. used this approach for the rapid extraction, preconcentration, and mixing of microRNA and reporters using ITP [71]. The total analysis time was 15 min and required only 5 ng of total RNA and obtained over 1000-fold improvement in sensitivity and 200-fold improvement in analysis time when compared with northern blotting, and a tenfold improvement in analysis time over RT-PCR.

All of the above work was performed using solution-phase hybridization. Karsenty et al. performed a theoretical and experimental study of the acceleration of surface-based hybridization using ITP and obtained a two-order magnitude improvement in signal when compared with a standard flow through reaction [72]. A 107-fold improvement was obtained in ITP hybridization when 10 nM molecular beacon was used but the gain in signal was reduced to 12-fold when 100 nM concentration was used, which was consistent with the theory prediction. Using ITP-based techniques, and based on the model curves for interpolation, the LOD of the standard flow and ITP-based techniques found to be 15 nM and 150 pM, respectively, which is consistent with the gain in signal.

Since being introduced a few years ago [73–76], the use of ITP for the purification of DNA has gained significant attention, as it is a simpler method than the use of more traditional methods for DNA purification by SPE. This is exemplified by the work of Marshall et al. who demonstrated cells lysis, extraction, and purification within an integrated single channel designed for printed circuit board device chip [77]. A resistive heater and a temperature sensor were incorporated into the TE reservoirs and 180 mA was applied to the heater for 3 min to lyse the cells. An LOD of 500 parasites/μL was achieved, which is the minimum clinical relevant LOD. The same group then optimized the design of the chip for

purification of nucleic acid from 25 μL of a biological sample [78]. The chip incorporated a capillary barrier structure to facilitate robust sample loading. A recovery of 76–86% of salmon sperm DNA for 250 pg to 250 ng of DNA was obtained within 20 min, making it exceptionally competitive with SPE. Shintaku et al. simultaneously analyzed RNA and DNA from a single cell using ITP without enzymatic amplification and the total analysis time was <5 min [79]. This method successfully extracted cytoplasmic RNA from the lysed cells when a bipolar voltage pulse was applied within the microchip and the DNA remained in the nucleus. Rogacs et al. reported ITP for bacterial RNA extraction and purification from whole human blood [80]. In the study, *Pseudomonas putida* cells were suspended into healthy human blood, lysed, and purified by ITP. The detection limit was 0.03–30 cells/nL blood (3.16×10^4–3.16×10^8 cells/mL blood).

Strychalski et al. used gradient elution ITP (GEITP) for DNA purification from crude samples for human identification using STR analysis [81]. In GEITP, a controlled variable pressure driven counterflow (CF) was used to control the focusing interface position while excluding other particulate and contaminations from the capillary, which is useful as it can be used to prevent PCR inhibitors from focusing with the DNA. LIF signal was used for on-line DNA quantification during the focusing step and it was possible to measure 0.5 ng/μL of DNA in standards, clean buccal swab, and soiled buccal swab, indicating that this can also be used for simultaneous DNA quantitation. The GEITP-purified DNA was used for STR analysis and successfully amplified all 16 STR loci.

ITP is also suitable for the concentration of cells. Prest et al. used free-flow ITP for bacteria of *Erwinia herbicola* focusing [82]. While no LOD was reported, the method showed that the bacteria cells were collected within fractions 6–8 indicating that cells are focused into ITP band. Oukacine et al. used ITP with a wide bore capillary for bacteria analysis using a UV detector [83]. The current was decreased down to 2 μA and the injection time increased to 380 s at −15 kV resulting in an LOD of 3000 cells/mL, sevenfold lower than their previously reported method [84] Phung et al. reported the use of ITP with EKI under FASI conditions for bacteria analysis [85]. *Escherichia coli* was not lysed prior to analysis but was stained off-line at room temperature using Syto 9 for 30 min. With LIF as the detector, the LOD of *E. coli* was 135 cells/mL, which is 22-fold lower than that using UV detection [83] and is more specific due to LIF only detecting stained cells. Saito et al. used polymer-enhanced transient ITP (tITP) for separation and detection of the same bacteria species (Gram positive bacteria) using boronic acid functionalized squarylium dye and on-capillary labeling agent, and the LOD based on 3σ of the area of the blank sample was found to be 3.1×10^5 CFU/mL [86].

Because of the ability of ITP to concentrate traces components in high ionic strength samples, it is not surprising that ITP can be used as a stand-alone method for various applications for DNA, cells, proteins, organelles, and amino acids. It has been used for biogenic amines in meat samples [87] and alcoholic beverages [88], glutamic acid and aspartic acid in tomato juice [89], anions and cations in renal stones [90], and carboxylic acids in human serum using customized microchips for the Agilent Bioanalyzer 2100 [91, 92]. The use of additives such as cryptand 222 and 2-hydroxy-methylbutyric acid has been reported to improve the separation of alkali metals [93] and lanthanides [94], respectively.

In the field of microfluidics, paper is generating significant interest because of the ability to fabricate fluidic devices rapidly and cheaply, with the first reports of ITP on paper described in the 1970s [95–97]. Moghadam et al. demonstrated ITP on a cross-shape NC membrane [98] for the fluorescent dye Alexa Fluor 488. A 900-fold enhancement was obtained with 60% extraction from 100 μL sample. Given the rejuvenation of the paper as a substrate for microfluidics, it is likely that this approach will feature prominently in the future. In alternatively cheap microfluidic devices, Shallan et al. used a 3D printer for chip fabrication [99]. Various designs can be constructed using CAD software and be printed within an hour. A microchip for ITP was printed in <5 min costing <$1 in material cost. The printed chip had a 10 cm serpentine channel and was able to perform ITP of three different analytes suspended in the terminator in 5 min [99].

tITP is the terminology used to describe the use of a short ITP stage prior to a subsequent electrophoretic separation in the same capillary/channel—most typically ZE. Huang et al. studied simultaneous quantification of dCDP and dCTP within 6 min using tITP-CZE method [100]. The injection time could be increased 150 times without a decrease in resolution and the sensitivity was enhanced up to two-order magnitude with the method. Wang et al. reported the use of SPME with tITP for CE-MS/MS using high-sensitivity porous ESI sprayer for proteomic analysis [101]. The results show that this approach was three times more effective in identifying proteins. Honegr et al. used tITP followed by CZE for preconcentration and determination of seven phenolic acids with the detection limit range obtained from 11 ng/mL (protocatechuic acid) to 31 μg/mL (syringic acid) [102]. The authors used SPE to clean samples prior to analysis to improve repeatability. Heemskerk et al. reported tITP coupled with porous sheathless interface MS in a neutral capillary to improve the sensitivity in glycopeptide analysis [103]. From the study, when a larger volume injection (37% of capillary volume) was used on a neutral coated capillary for tITP-CZE and interfaced with MS, 40-fold increase in sensitivity was obtained for IgG1 Fc glycopeptide analysis when compared to conventional strategy. tITP was coupled with MEKC in CZE for analysis of 3-nitrotyrosine in urine by Ren et al. [104]. A peak efficiency up to 1 000 000 was obtained for tITP in MEKC and obtained a fourfold improvement in sensitivity when compared tITP in CZE and an LOD in urine of 0.07 μM. Matczuk et al. reported the use of tITP-MEKC to concentrate neutral analytes from high-conductivity samples with tenfold and higher enrichment factors [105]. The detection limits of five metallodrugs used in this method were in 10^{-7}– 10^{-8} M range for hydrophobic compounds.

In pseudo-ITP (pITP), organic solvents are used as terminating electrolyte, which was first reported by Shihabi

[106–108]. One of the advantages of pITP is the very less sample preparation time and it has been reported for number of analyses such as biogenic aminothiol, drugs, and peptides in biological samples [109]. Dziomba et al. reported the use of FASI with p-ITP for the determination of seven psychiatric drugs in human urine samples after liquid–liquid microextraction [109]. SEFs (8000–13 400) and LOD (1 ng/mL) were obtained when compared to a typical hydrodynamic injection.

In the previous review, the introduction of depletion zone ITP (dzITP) by Quist et al. was highlighted as an interesting approach to sample treatment because it leverages CF gradient focusing to create a depletion zone using only a single electrolyte. Since then, the authors used this approach with a novel filtering principle in combination with dzITP [110]. The filtering method is based on the balance of fluxes such that selectivity can be obtained as the dzITP orders compounds into distinct zones before they pass the depletion zone. In this study, two modes of filtering were used: continuous and pulsed. In the continuous mode, the supply, focusing, and separation are synchronized with a continuous flow of compound released resulting in trapping other specific compounds. In the pulsed mode, voltage pulses allow the release of discrete zones. Sample mixtures containing 100 μM fluorescein and 400 nM 6-carboxyfluorescein with 100 μM sodium acetate as an intermediate spacer zone were used to study the performance of these two approaches. The use of filter for dzITP provides a fourfold enhancement in the detection of 6-carboxyfluorescein even though the concentration is 250× lower than the starting concentration.

2.1.4 CF gradient focusing and electrocapture

CF gradient focusing encompasses a range of techniques (electric field, temperature, micelle, etc.) that rely on a local electric field generated within the separation space to focus individual samples based on their electrophoretic mobility within the separation channel. As mentioned in previous review, full details on the various mechanisms within counter flow gradient focusing (CFGF) and their applications can be found in reviews by Shackman and Ross [111], Meighan et al. [10], and Fosdick et al. [112].

In the last review article, Crooks' group had just introduced bipolar electrode focusing for enrichment to focus anions [113–115]. Sheridan et al. reported bipolar electrode focusing for cations, in which the EOF was reversed by coating with a monolayer of polybrene. Using a model cationic dye, enrichment in Tris-HCl was similar to the previous results for anions [113, 115] but a higher voltage was required because of more significant depletion of the Tris-H^+, which made the system less stable due to the formation of O_2 and H_2 gases at the electrode surface. Knust et al. reported the use of two parallel microchannels connected with a bipolar electrode for simultaneous enrichment and separation of both anions and cations in a single microchannel [116]. Tris-H^+ is neutralized by OH^- at the cathodic end of the electrode, while acetate buffer is neutralized by H^+ at the anodic end. This generates an electric field gradient in the bottom channel on which the anions and cations are focused and separated. A hydrodynamic pressure-driven flow (opposing CF) was required for enrichment due to the absence of EOF. This allows the cations to be enriched on the left with an SEF of 136, while anions being enriched on the right with an SEF of 113. In subsequent work, Scida et al. developed an electrochemically gated method for enrichment, separation, and delivery of the enriched ions into a different secondary microchannel [117]. First, a voltage of 30.0 V was applied between the connected poles of BPE 1 allowing the enrichment of $BODIPY^{2-}$ (green) and $MPTS^{3-}$ (blue) in the primary channel. The deactivation of BPE 1 and activation of BPE 2 lead to the opening of the electrochemical gate at SC1 allowing $BODIPY^{2-}$ to enter the SC1 channel, and the deactivation of BPE 2 and activation of BPE 3 allow the electrochemical gate to be open at SC2 allowing $MPTS^{3-}$ to enter. However, when BPE1 is activated at $t > 30$ for the enrichment of $BODIPY^{2-}$, the $MPTS^{3-}$ band was observed to move backward occasionally into the anodic reservoir. This is due to the large ΔE_{elec} rising from the angled geometry of the BPE gating. The EF of $BODIPY^{2-}$ was 3.1 ± 0.1 after 26 s and $MPTS^{3-}$ 27 ± 2 after 56 s with the rate of enrichment calculated to be 0.11-fold/s and 0.31-fold/s for $BODIPY^{2-}$ and $MPTS^{3-}$, respectively [117].

While Crook's group introduced the use of planar microchip design for BPE focusing, Cao et al. introduced the use of microchannel plate for 3D BPE focusing of anions [118]. Figure 3 shows the SEM images of the sectioned microchannel plate and the schematic on how it can be used for BPE of anions enrichment. The thousand microcapillaries act in unison as tiny BPEs due to the semiconducting sidewall and high aspect ratio structure. Using this, they managed to obtain an enrichment of 13 400-fold (70 s) using a voltage bias of 800 V.

Temperature gradient focusing exploits the dependence of electrolyte/ion properties on temperature and was originally introduced by Ross and Locascio [9]. The most recent work is by Shameli et al. who used micellar affinity gradient focusing in a microfluidic device for bilinear temperature gradients study [119]. Bilinear temperature gradient consists of two gradients: a steep gradient for focusing and a shallow gradient for separation. Two surfactants were used, SDS and poly-SUS, and the resolution of fluorescent p*I* markers was improved by 2 and 1.6, respectively, over a linear gradient. Han et al. reported a numerical study of using joule heating for temperature gradient focusing on the effect of the microchannel geometry [120]. From the numerical study, the focusing performance can be improved using a narrow middle width with a wider outside width of the channel with the w_{mid}/w_{out} of 0.075.

Electric field gradient focusing uses an electric field gradient electric field to focus ions where their electrophoretic velocity is balanced by a hydrodynamic flow. Trickett et al. reported the use of a polyaniline electrode with varying width from 200 to 5000 μm in 320 μm increments, providing a 20-fold resistance change [121]. The novel electrode, however, showed only modest performance, separating and concentrating R6G and Q by threefold within 10 min.

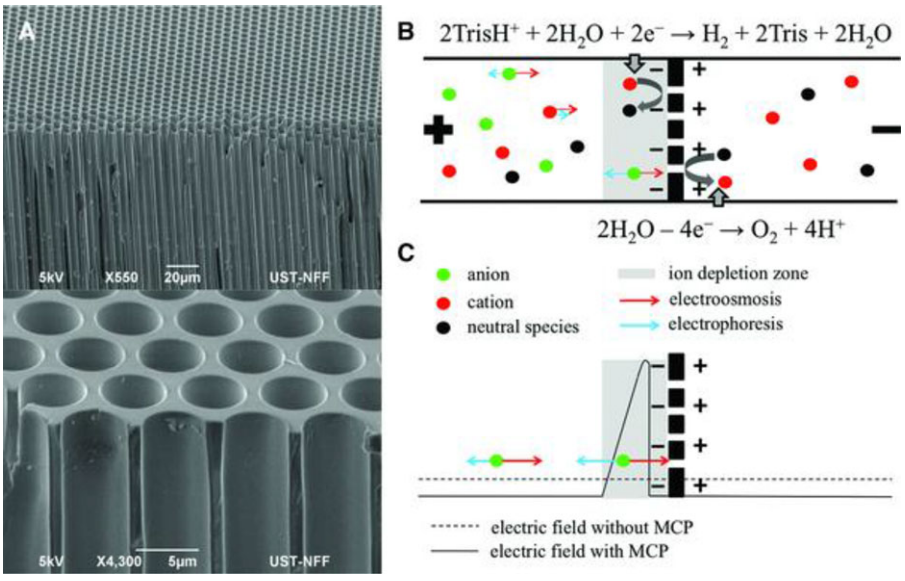

Figure 3. (A) SEM images of a sectioned MCP depicting densely packed microcapillaries. (B) Schematic description of the microdevice for bipolar electrode enrichment of anionic species whereby faradaic depolarization drives MCP into cathodic and anodic poles following the stated reactions and leads to an ion-depleted low-conductivity zone (the shaded zone) next to the cathodic surface. In the zone, cathodic electroosmosis balances out anodic electromigration as represented by the arrows, the velocity vectors acting on the ionic species. (C) Rendering of the local electric field distribution along the channel with (solid line) or without (dashed line) faradaic reactions. Reprinted with permission from [118].

In gradient elution moving boundary electrophoresis, the electrophoretic migration of the analytes is opposed via a bulk CF with the magnitude of the flow slowly reduced sequentially allowing ions with different mobilities to enter the channel at different times [122]. Ross' group used FASI with gradient elution moving boundary electrophoresis, and with a conductivity ratio of 8.21, an SEF of over 100× was achieved. They were also able to demonstrate the detection of arsenate [123]. One of the more interesting outcomes, however, was the concentration of ions outside the microchannel as a result of the CF, an idea that has been discussed several times, but experimentally shown for the first time here.

2.2 Chemically induced changes in velocity

2.2.1 Dynamic pH junction

In this approach to stacking, a pH interface between the BGE and sample is created, which changes an analyte's ionization state leading to significant alteration of electrophoretic mobilities, which causes concentration and focusing [124]. In the late 1990s, this was termed dynamic pH junction by Britz-McKibbin et al. [125], but is also known as a moving neutralization boundary [126] and is a subset of moving reaction boundaries [127].

Zhang et al. developed a sensitive and environmentally friendly method for 2-nitrophenol, 3-nitrophenol, and 4-nitrophenol separation. Using a high-pH BGE (borate) and low-pH sample (acetate), enhancements of 60–90 were obtained giving LODs between 2.7 and 8.7 μg/L. The method was applied to tap and fishpond waters with the only the preparation required being adjustment of the sample pH [128]. Biogenic amines are found at extremely low concentrations in biological fluids, for example the normal values of dopamine, epinephrine, and serotonin in human urine are in the range of 37–343, 0–14, and 150 ng/mL, respectively, and are difficult to detect by classical methods. Tang et al. used dynamic pH junction with CE and amperometric detection and significantly, their method does not require any sample pretreatment or derivatization. As it can be applied to urine, it may be useful for clinical diagnosis as high urine concentrations of dopamine and norepinephrine are correlated to pheochromocytoma [129].

One of the advantages of dynamic pH junction is that it works with high ionic strength samples. However, Hsieh et al. noticed that while increasing the ionic strength of the phosphate sample buffer and borate BGE buffer to over 40 mM, it led to deterioration of 5-aminolevulinic acid focusing, in which the peak became broader and its height lowered significantly. They attributed this to the mismatch of conductivity between the BGE and sample matrix. In order to overcome this issue, the sample matrix conductivity was adjusted to be lower than that of the BGE. With this dilution, very good sensitivity improvement of about 50-fold and an LOD of 1.0 mg/mL were achieved through prolonged sample injection up to 10.4% of capillary length [130].

If the sample has a pH difference as well as a conductivity difference, then it is possible to combine both pH junction and FASS/FASI for further enhancements. This was examined by Acosta et al. for seven phenolic compounds in herbal products commercialized in Argentina. FASI was examined but due to quantitative limitations with long injection times due to the biased injection of species with a higher electrophoretic mobility, they concluded that hydrodynamic injection would be more appropriate. The optimum injection length was 50 s (31%). [131].

Zhu et al. reported dynamic pH junction technique for bottom-up proteomics analysis [132]. For a BSA digest, they found that the sequence coverage increased to 70% with more than 40 peptides identified with pH junction of 0.05 mg/mL compared to 66% coverage and 37 peptides identified with a conventional injection of 1 mg/mL. When applied to whole *E. coli* digests, the dynamic pH junction base peak intensity

was 20 times greater, than with a normal injection, and as shown in Fig. 4, a significant increase in resolution was also obtained. Additionally, superior results for dynamic pH junction were obtained when compared to FASS.

2.2.2 Association with pseudophases

Terabe et al. [133, 134] originally introduced MEKC as a mode of CE developed to analyze neutral compounds by SDS micelles as pseudostationary phase. A decade later, pseudostationary phases evolved into being used in preconcentration mechanisms by virtue of their interaction with the compound of interest. The most prominent stacking techniques that employ pseudostationary phases are sweeping [135, 136], analyte focusing by micelle collapse (AFMC) [137, 138], and micelle to solvent stacking (MSS) [139]. The search via Scopus showed 33 research papers within the review period.

2.2.2.1 Sweeping

Sweeping was initially developed by Quirino and Terabe to increase detection of neutral and charged analytes in MEKC with samples having the same conductivity as the BGE [135,136]. The technique involves the injection of sample solution devoid of the pseudostationary phase. When the electric field is applied, the micelles present in the background solution penetrate the sample zone, and subsequently pick and accumulate the analytes into a narrow band. The enrichment of the analytes is largely dependent on the analyte–micelle interaction, described by the chromatographic retention factor *k*. Since its introduction 15 years ago, sweeping has grown to be one of the most prominent and universal concentration systems in the field because of its applicability to both charged and neutral species and its tolerance of high ionic strength samples. Papers will be discussed below based on the conductivity of the sample solution with regard to that of the BGE.

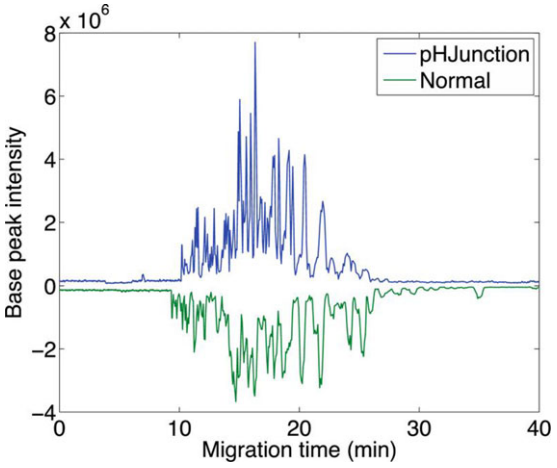

Figure 4. Base peak electropherograms for a 20 nL injection of a 0.1 mg/mL *E. coli* tryptic digest. The blue (top) represents the electropherogram generated using a pH junction injection, and the inverted green (bottom) represents electropherogram generated using normal injection. Reproduced from [132] with permission.

When the sample has a lower conductivity than the BGE, the combined effects of two focusing steps, sweeping and stacking, affect the preconcentration of the analytes. When voltage is applied, the micelles in the BGE traverse through the sample solution and sweep the analytes. Sample stacking at the stacking boundary focuses the swept zone further [136]. Six papers used sample solutions with a lower conductivity for the stacking and separation of charged analytes in sweeping [48, 62, 140, 141]. SDS was used as the pseudostationary phase for all papers. Enhancement factors in the range of 31–300 allowed the successful determination of the analytes of interest in human serum/plasma, bacterial growth medium, urine, and medicinal product.

Focusing of analytes prepared in a sample solution of equal conductivity to the BGE is affected by sweeping alone. Five papers used these conditions, four of which employed neutral analytes and SDS as the pseudostationary phase [142–145], while one used charged analytes and anionic sulfated-β-CD as the pseudostationary phase [146]. After optimization of the stacking methods, about 25- to 2500-fold increase in sensitivity compared to normal MEKC was attained. The developed methods were successfully applied to the analysis of steroids in urine, herbicides in cereal and vegetable samples, and water samples.

A new development to sweeping was developed by Rabanes et al. for the determination of charged alprenolol enantiomers in the presence of high organic solvent in the sample solution [146]. The interaction of analytes with the sulfated-β-CD is low in the sample solution due to the organic solvent. The analytes electrophoretically migrated from the sample in the opposite direction to the CD and are concentrated as a result of the interaction with the CD in the aqueous BGE zone. This is in contrast to conventional sweeping mechanism, wherein analyte focusing occurs at the front of the pseudostationary phase as it moves through the sample zone. An SEF of more than two orders of magnitude was obtained when the sample was introduced electrokinetically for the chiral separation of alprenolol enantiomers in standard solutions.

The effect of high-conductivity sample solution in sweeping had been theoretically and experimentally studied by two groups [147, 148] in the early 2000. El-Awady et al. recently revisited the theory on the effect of high-conductivity sample solution in sweeping [149]. They found that the sweeping efficiency of neutral analytes is independent of the conductivity of the sample solution. In a sample with a higher conductivity than the BGE, the low electric field of the sample causes the micelles to stack at the sample/BGE boundary and the stacked micelles sweep the analyte from the high-conductivity zone. The higher the ratio of conductivities of the two zones, the more micelles are stacked and the better sweeping occurs. Thereafter, the stacked micelles and swept analytes migrate into the low-conductivity BGE zone and adjust to the low Kohlrausch function in this region, thus destacking occurs.

The extent of the stacking and destacking is equal, thus the focusing of the analytes is only contributed by sweeping, as was originally proposed by Quirino and co-workers [157].

El-Awady and Pyell presented a theory of independent effects of sweeping and retention factor gradient designed to be able to assess sweeping efficiency in homogeneous and inhomogeneous electric field conditions [150]. Specifically in this work, organic solvent in the sample and BGE was used to adjust the retention factor in the BGE and sample, and they demonstrated that sweeping efficiency is influenced by both retention in the sample and BGE. For example, when k_{sample} is higher than k_{BGE}, when the swept zone of analytes enters the BGE zone, the electrophoretic mobility decreases because of a decrease in retention caused by the presence of organic modifier in the BGE. An opposite phenomenon occurs when k_{BGE} is higher than k_{sample}. In their work, however, the additional experimental defocusing/focusing factor was in the range of 0.81–1.53 and the experimentally obtained k_s and k_{BGE} are not significantly different, thus drastic focusing/defocusing is not evident.

Modir-Rousta and Bottaro [151] developed a pressure-assisted sweeping method for the determination of polar neutral *N*-nitrosamine compounds. The auxiliary pressure aided in the introduction of polar neutral analytes in conditions where there is no EOF, thus decreasing the analysis time and allowing the use of longer capillaries for larger sample volume injection. LODs of at least 0.11 mg/L were achieved.

2.2.2.2 MSS and AFMC

MSS and AFMC rely on the release of captured analytes from the micelle before detection. This phenomenon is due to the presence of organic solvent (a plug or with the sample solution) for MSS or a zone in the capillary that decreases the CMC of the micelles for AFMC. Six papers were found to apply MSS as a stacking mechanism, five of which used SDS as a pseudostationary phase for the analysis of cationic analytes [152–156] and one used CTAB for anionic analytes [157]. One paper was found to use AFMC as stacking mechanism [158]. SEFs of 12-to 6300-fold were achieved. The developed methods were successfully used to elucidate nitroimidazoles in rabbit plasma, alkaloids in human plasma, herbicides in fortified drinking water, berberine and theophylline in urine, antipsychotic drugs in spiked wastewater, and alkaloids in Chinese herbal medicine.

Quirino and Aranas [152] modified the original MSS configuration by introducing a micellar solution before hydrodynamic injection of the sample, which contained at least 30% organic solvent. The introduction of micellar solution before the sample plug eliminates the effect of field-enhancement and pITP. The presence of organic solvent in the sample solution accommodates the analysis of sample matrices with high salt concentration and is ideal for samples pretreated with organic solvents, through protein precipitation, or the extract from SPE. The developed method was applied to six cationic antipsychotic drugs in wastewater with SEFs between 41 and 68.

Instead of MSS or AFMC, Shuli et al. described a transient moving substitution boundary method [159] that has many parallels to these two approaches and thus has been included here. Their stacking system used crown ethers (18-crown-6-tetracarboxylic acid (18C6H4)) as a pseudostationary phase to transport, release, and accumulate analytes at a substitution boundary. A schematic is shown in Fig. 5, in which Na^+ is used to displace the analytes. An SEF of up to 940 for aminoglycoside antibiotics was reported.

2.3 Physically induced changes in velocity

Ion-selective membranes and nano/microchannel interfaces (NMIs) introduce unique phenomena that in some case dictate the behavior of the entire microfluidic system. Nonequilibrium ion current phenomena include ion concentration polarization associated with the formation of depletion and enrichment zones, current rectification, water splitting, and many others that can be used for extraction, concentration, separation, and detection of biomolecules [160]. Ion selectivity of an NMI is the result of the nanochannels pore size and surface charge density as well as the bulk medium ionic strength and pH.

Once a channel is filled with electrolyte solution, and electric double layer (EDL) develops on the surface with the counterions closely packed in the Stern layer followed by a diffuse layer containing co-ions. Applying an electric field across the channel creates EOF by dragging the counterions near the wall toward the cathode in the case of negatively charged walls. It is generally agreed that EOF significantly affects NMI with nanochannels (>10 nm). The role of buffer ionic strength intensifies in nanochannels as the EDL approaches the radius of the nanochannel and two cases can be identified. Complete overlap leads to charge-governed transport, in other words, the surface co-ion will be excluded and there is enhanced transport of the counterion. Incomplete overlap leads to size- or geometry-governed transport as a free-transport region still exists, surrounded by the electrostatic region, and through which the co-ion can be transported if the hydrodynamic size fits through the free-transport region. The extent of the EDL, Debye screening length, is affected by the charge density of the walls and the pH and ionic strength of the bulk solution. Complete overlap is not necessary to induce ion selectivity as some highly charged surfaces retain their permselective properties even in high ionic strength solutions when the EDL is suppressed.

Ion concentration polarization (ICP) occurs when there is preferential transport of counterions and expulsion of co-ions. To preserve electroneutrality on both ends of the nanochannels, anions are depleted on the anodic side and concentrated on the cathodic side. Protein trapping with NMI while continuously injecting the sample was achieved in 85-nm-deep nanochannels connecting two microchannels with different pH and filled with protein-buffer solution pumped at 1000 nL/min flow rate [161]. The low-pH microchannel was connected to the positive electrodes and the

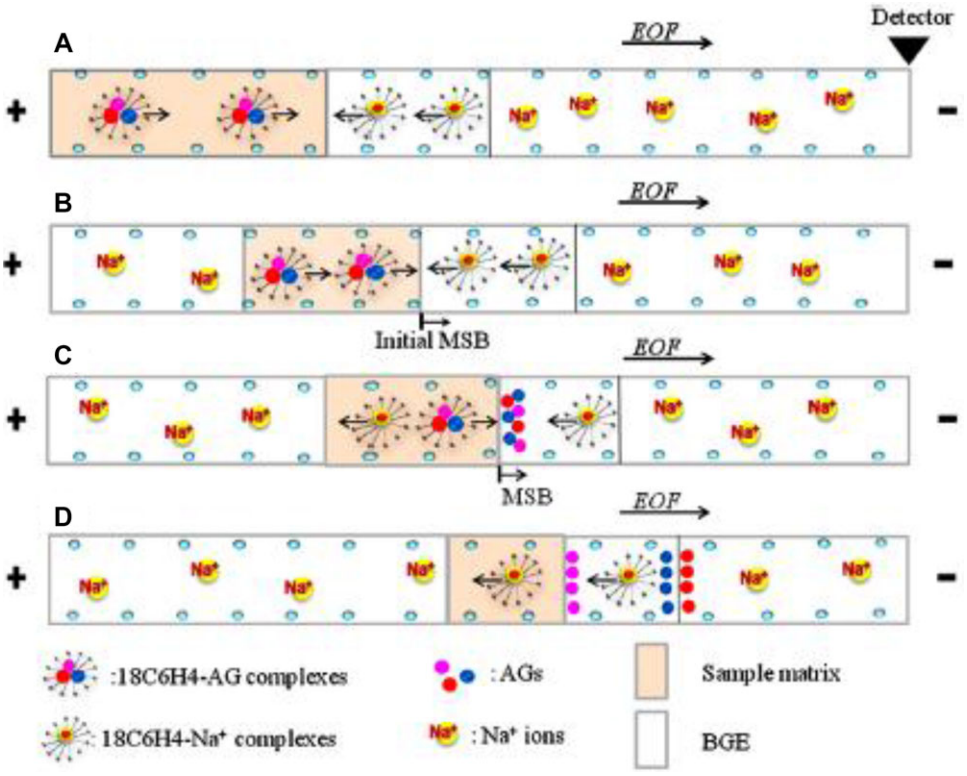

Figure 5. Schematic illustration of the on-line concentration with the FESI-moving substitution boundary method: (A) starting situation of FESI with PSP plug and sample plug injected electrokinetically, (B) sample zone gets stacked under the electrical field, (C) focusing by moving substitution boundary principles, (D) CZE separation of the focused anlaytes. Reproduced from [159] with permission.

high-pH microchannels to the negative electrodes. Enhancements were 385-fold for R-Phycoerythrin within 10 min and 107-fold for Dylight-labeled streptavidin within 3 min. The SEF for Dylight-labeled streptavidin was due to saturation of focusing as both proteins reach the same concentration in milligram per milliliters.

Most stacking methods do not work in high ionic strength samples, which is also a problem for ICP methods but they can be modified to overcome this limitation by increasing the surface charge of the nanochannel or by decreasing nanochannel pore size. The main problem in doing this is the stabilization of the depletion and enrichment zones because the formation of vortices near the NMIs leads to mixing and limits the SEF that can be achieved. To help determine the optimal conditions, an electrical resistive circuit network model was designed to predict the optimum applied voltages and to precisely position concentrated protein bands at certain distance from the NMI [162]. Experiments showed more than 10^5-fold enhancement within 5 min using 1 mM phosphate buffer and nanochannels etched in glass and sealed to PDMS slab.

2.3.1 Effect of channel geometry

Microchannel geometry was found to affect enrichment factors and the time needed to reach saturation [163]. In straight channels, the depth did not affect the maximum enrichment factor achieved but the deeper channels required longer time to reach saturation: a 100-fold enrichment of fluorescein in 50-μm-deep channel required 420 s compared to only 90 s when it was 6 μm deep. In convergent–divergent channels (15 μm deep), 200-fold enrichment was achieved within 150 s using the same hydrogel NMI. Similar results were obtained using hydrogels and Nafion™ membranes.

Concentration gradients were generated in straight and tapered nanochannels connecting two different conductivity solutions, 6 μM on one end and 2000 μM at the other end [164]. The difference in concentration between the two ends created chemiosmotic flow toward the low-concentration end that dominated the EOF at low applied voltages. In straight channels, when the flow direction is opposite to the concentration gradient, the electric field increases sharply at the low-conductivity end and forms stable traps so that particles can be trapped at a certain location. This does not happen if the flow is in the same direction as the concentration gradient. In tapered nanochannels, the narrower end is at the high-conductivity side, which means that the electric field will increase on both sides. The simulation curves presented imply that the more tapered nanochannels, 1:9 width ratio between the high- and low-conductivity ends, will give better separation of trapped particles based on charge-to-size ratio.

2.3.2 Fabrication methods

NMI can be incorporated into microfluidic devices using different fabrication approaches that vary in cost, time, success rate, and compatibility with mass production. While some are very promising to be developed into commercial point-of-care

devices, others are important in understanding the behavior of NMI and unravel more about their unique phenomena.

Studies comparing the behavior of different NMI materials facilitate selecting the most appropriate for a particular application. Kim et al. compared four different membranes regarding their ease of fabrication, robustness, biocompatibility, and charge density [165]. Two separate microchannels were connected with a third channel that was filled with the nanoporous material. Nafion™, agarose, and anion- and cation-selective hydrogels were compared with Nafion™, and agarose membranes were easier to fabricate reproducibly but the hydrogels offered better flexibility to manipulate the surface charge. Nafion™ membranes offered the fastest concentration rate but the agarose hydrogel was better suited for concentrating bio-samples as agarose does not have sufficient surface charge to support EOF and negatively charged proteins at physiological pH will migrate toward the anode only by the effect of electrophoretic mobility.

While most preconcentrators are optimized for anions, cationic preconcentrators are also useful when the separation is done in acidic buffer conditions below the p*I* of the proteins and they are positively charged. Shin et al. compared three methods for creating cation preconcentrators in glass chips under reversed EOF conditions [166]. An anion permselective poly(diallyldimethylammonium chloride) (PDADMAC) membrane was photopolymerized between two *N*-[3-(trimethoxysilyl)propyl]-*N′*-(4-vinylbenzyl)ethylenediamine hydrochloride (TMSVE)-coated microchannels or 40-nm nanochannels were etched and then coated with cationic monomers, TMSVE or polyE-323, to impart a positive charge on the surface. In 0.005% formic acid + 5% IPA at pH 3.4, concentration factors of R6G were just below 15-, 30-, and 40-fold for PDADMAC, TMSVE, and polyE-323 nanochannels, respectively. When 1 mM phosphate buffer, pH 7.4, was used, the PDADMAC performance deteriorated but the other two concentrators did not seem to be affected. When 10 mM phosphate buffer at the same pH was used, PDADMAC showed stable preconcentration due to the surface charge increase with the ionic strength and the pore size was small enough to maintain EDL overlap. However, the coated nanochannels, 40 nm, failed to concentrate as the EDL overlap was not achieved at the higher concentration of the buffer. Regarding applied electric fields, the coated nanochannels were more robust and tolerated higher electric fields and were less prone to peptide adsorption than the PDADMAC membrane.

Nanochannels were realized in polycarbonate substrate by UV exposure at 254 nm in presence of O_2 and then reversibly sealed to PDMS slab to sequentially concentrate, label, and purify BSA (Fig. 6) [167]. Using optimum nanochannel depth of about 45 nm and 20 mM bicarbonate buffer, pH 9.0, enrichment for 300 s resulted in 10^2- to 10^3-fold enhancement at the anodic side of the nanochannels. The voltage was switched to the FITC reservoir to deliver FITC through the concentrated protein zone and the excess FITC migrated through the nanochannels to the auxiliary microchannel. A purification step was then maintained for 90 s

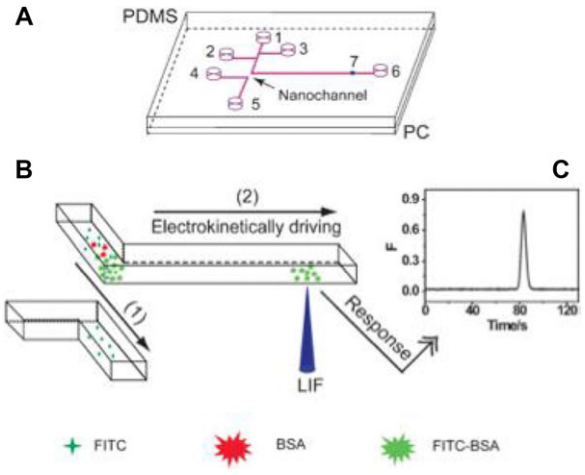

Figure 6. (A) Schematic illustration of the micro/nanofluidics device for FITC labeling of protein. The nanogap is indicated by an arrow; (1) FITC reservoir; (2) BSA reservoir; (3–6) buffer reservoirs; (7) laser-induced fluorescence detection point. Total length 1–6 = 40 mm. (B) Schematic illustration of the principle for FITC labeling of proteins on the micro/nanofluidic device using BSA and FITC as model systems. (1) The electric field for protein concentration and FITC labeling; (2) the electric field for product separation and detection. (C) Corresponding fluorescence response of the purified product (FITC–BSA). Reproduced from [167] by permission of The Royal Society of Chemistry.

by switching the voltage to the buffer reservoir to remove all unreacted FITC before the separation voltage was applied. The enrichment of the protein enhanced the reaction rate by factors of 10^4- to 10^6-fold compared to bulk solution labeling, which takes 14 h. This is a very simple and intelligent use of ICP to concentrate and purify proteins and then to derivatize them and will help in the creation of simple and portable devices for protein measurement.

2.3.2.1 Nafion™ membranes

Nafion™ membranes can be integrated in microfluidic devices to form an NMI but control over pore size is difficult and problems such as leaking and membrane deformation limit their use. Major problems are instability of the formed ICP, membrane deformation at high applied electric fields, and leaks due to inadequate sealing.

End-labeled free-solution electrophoresis of DNA was achieved simultaneously with more than 10^3-fold enhancement within 240 s [168]. A 100-μm Nafion™ film connecting the sample and buffer microchannels acted as an NMI, which created depletion forces to balance the opposing EOF and trap streptavidin-bound and biotinylated-free DNA, in 5 mM Tris-HCl buffer, at different locations along the sample microchannel, resolution achieved was 1.85.

Kim et al. argued that ICP observed in channels near Nafion™ membranes could be due to hidden triangular nanochannels created by incomplete sealing between PDMS and glass near the Nafion™ membrane [169]. They augmented the argument by presenting results from devices fabricated in the same way often reported in literature with that of

a device where complete sealing was ensured. Most of the ion transport seems to be through the triangular channels rather than through the Nafion™ membrane. Depletion zones were observed using fluorescein for Nafion™ membranes and nonconducting membranes and with varying conditions of membrane thickness (100 and 500 nm) and different ionic strength of the bulk solution. The transition of ionic transport from surface charge governed to geometry governed was attributed to the bulk ionic strength that determines whether EDL overlap occurs or not.

An easy way to incorporate Nafion™ membranes without gaps was reported by Zhang et al. for concentrating DNA by 10^3-fold within 15 s [170]. A fracture, 650 nm, was made in the wall of fused silica capillary and filled with Nafion™ at equal distance from both ends. A reservoir was attached above the Nafion™ membrane and connected to positive voltage while the two reservoirs at the ends were connected to negative voltage. Concentration of the DNA was achieved at the cathodic side of the membrane using relatively high voltage of 800 V without deformation of the membrane.

Surface-based immunoassay sensitivity was enhanced by 500-fold for C-reactive protein, a disease marker with many different clinical applications [171]. The difference in conductivity of the Nafion™ membrane and the microchannel creates depletion zone near the membrane, the length of which decreases by increasing the ionic strength of the bulk solution, resulting in better preconcentration. However, ionic strength as high as 1× PBS induces instability in the concentrated zone and decreases the preconcentrator efficiency. Experiments show that higher enhancement factors were achieved by increasing the membrane width and thickness and by the electric field strength.

A million-fold enhancement was reported for FITC-labeled BSA in 1 mM PBS within 60 min also using Nafion™ membrane in an open channel [172]. Bacterial cells that express green fluorescent protein (GFP) were also concentrated on the depletion zone border accompanied with cell lysis due to osmotic pressure difference between the cell and buffer at the boundary. Different concentration bands were observed for the bacterial cells and GFP as a result of differences in their electrophoretic mobility. The high-concentration factors achieved can be attributed to the use of single open channel design instead of the dual closed one. Besides avoiding leaks, minimized Joule heating and increased bulk flow lead to rapid formation of ICP zone that can be maintained for 60 min at relatively high applied electric field (25 V/cm) without membrane deformation.

For the first time, depletion zone created near Nafion™ membrane in an open channel was used to continuously separate micro- and nanoparticles based on differences in electrophoretic mobility [173]. The particles were delivered to the depletion zone by hydrodynamic flow from a narrow side channel (Fig. 7). The movement of the particles along the channel is governed by the balance between the hydrodynamic and electrical forces. Higher applied electric fields across the membrane lead to shift in the path of the particle to a region where hydrodynamic force is dominant resulting in wider deflection angle and even complete block of transport. The contribution of dielectrophoresis was negligible compared to the electrophoretic mobility and particles with higher mobility were deflected at wider angle regardless of their size and hence separation is attributed to differences in electrophoretic mobility. Compared to conventional free-flow electrophoresis, this method utilize high electric fields near the NMI without the need to use internal electrodes making it simpler and less prone to bubble generation. Yet, the dispersion of separated bands, especially nanoparticles, is a limiting problem. The experiments were done using fluorescent polystyrene particles in 1 mM dibasic sodium phosphate but the authors expect that applications may extend to include separating biomolecules, DNA, cells, and even ions.

Myoglobin, an early indication of myocardial infarction, was trapped at NMI to achieve 10^3-fold enhancement within 200 s starting with 1 ng/mL solution in phosphate buffer (pH 7, 10 mM) [174]. Labeling with Alexa fluor 488 imparts a weak negative charge and enables the electrokinetic trapping. Using microflowing technique that allows patterning of thin layer of Nafion™, a 200-nm-thick bridge between a microchannel filled with the protein to another filled with buffer served as the nanojunction.

2.3.2.2. Hydrogels

Hydrogels offer a wide range of physical and chemical properties and can be incorporated into a microfluidic device in a specific position through thermal- or photopolymerization.

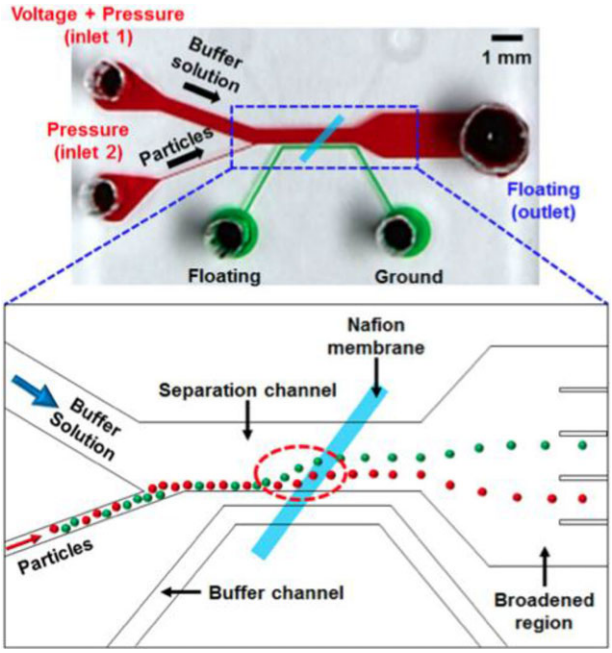

Figure 7. Schematic diagram of the separation device and separation process (microchannel: PDMS; nanojunction: nafion membrane; microchannel height: 40 μm. Different colors represent particles having different properties; the red dotted circle denotes the ion-depletion region). Reprinted by permission from Macmillan Publishers: [173], copyright 1993.

Surface charge density and stability over a wide pH range can be tuned by the proper selection of monomer, while pore size can be tuned by controlling the cross-linking process.

To accurately position a hydrogel plug, Lee et al. employed the elasticity of PDMS to hold the hydrogel during photopolymerization [175]. Two air channels with thin PDMS base were used to apply pressure and the deflected PDMS film prevented the spread of the monomers until photopolymerization was complete. The hydrogels were used to trap and release DNA and cells.

Increasing the nanopore density, with associated decreasing pore size, of polyacrylamide gels resulted in higher enrichment factors and 600-fold was achieved for FITC within 120 s and stable enrichment zones were maintained even at relatively high applied voltage of 300 V [176].

Han et al. increased the sensitivity of extraction of negatively charged hydrogel by combining it with bead-based competitive immunoassay for small molecules such as biotin and achieved 2×10^3-fold enhancement in 3 min [177]. Anionic fluorescent indicator was quantitatively replaced from magnetic beads by the unlabeled analyte and preconcentrated near the depletion zone created at the NMI.

2.3.2.3 Elastomers

PDMS enables low-cost fabrication of nanochannels because of its ability to stretch and deflect under applied force. Ultrahigh aspect ratio nanochannels were made in PDMS by casting over a template containing parallel bumps (2–4 μm high) and then rolling the PDMS layers after curing to have the nanochannels in between the layers of the roll (Fig. 8) [178]. Stretch and release during the fabrication process enabled tuning of the nanochannels size and shape. Plasma treatment ensured irreversible binding and the roll was mechanically cut into discs according to the desired length. The disc was then sandwiched between two layers containing the microfluidic channels. However, the nanochannels diameter was around 700 nm, which is considered very large compared with other nanofabrication techniques.

Alternatively, by applying a high pressure over a thin PDMS film, a small gap, nanometer size range, is left, which can support ICP. Quist et al. demonstrated anodic and cathodic enrichment by manipulating the applied pressure to switch between the two modes [179]. After reasonable concentration was achieved, the pressure was released to allow the concentrated plug to pass through for subsequent separation. A 10^3-fold enhancement of fluorescein was achieved in 100 s. One of the disadvantages noted in this work is the somewhat lower efficiency of the plug that passes through the opened channels.

2.3.2.4 Dielectric breakdown

Dielectric breakdown of PDMS is 21 V/μm, above which PDMS starts to fail and develop nanofissures. We developed a method to control the pore size of the nanojunctions formed between two microchannels using slightly higher electric breakdown voltage of 22 V/μm over a 100-μm gap [180]. Different permeability ranges were achieved by setting a current limit during the breakdown to lower the applied voltage once the nanojunctions are formed. When the current limit is set at higher value, the applied voltage will continue for longer until the nanojunction pore size is wide enough and has a conductivity that matches the preset current limit. Direct extraction and analysis of quinine in whole blood was achieved in 3 min.

Later, another group reported nanoparticle-assisted breakdown for protein concentration [181]. The main microchannels were 2 μm deep and 100 μm wide and separated by a 40-μm gap. The part containing the channels was made of PDMS prepared in a prepolymer base to curing agent ratio of 5:1 to give a harder PDMS than the 10:1 ratio and prevent collapse of the channels. Gold nanoparticles (13.7 ± 0.8 nm), deposited at the gap before binding PDMS to glass, facilitated breakdown at much lower voltage of 7.5 V/μm. FITC-labeled

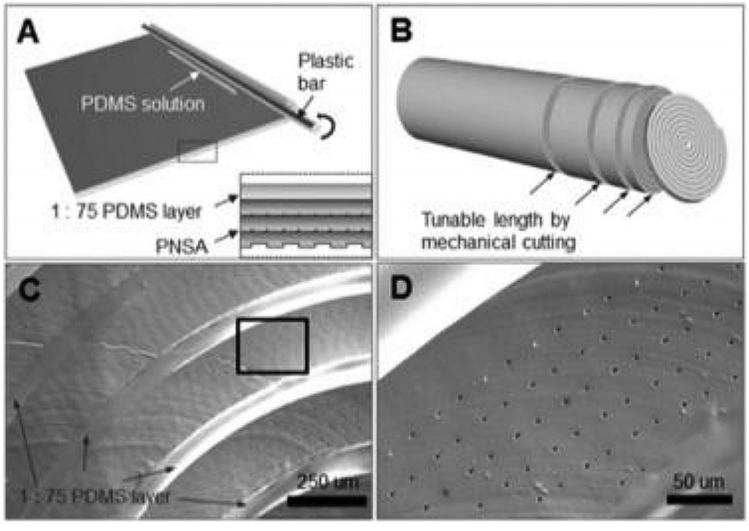

Figure 8. Large-area integration by PNSA rolling. (A) Schematic illustration of large-area integration using a sticky (1:75) PDMS layer. Magnified inset image showing a cross-sectional view before rolling. (B) Schematic illustration of the rolled PNSA structure; this structure can be mechanically cut on demand. (C) SEM image of the radially formed PNSA and PDMS films of 1: 75 weight ratio and (D) magnified view of (C). Reproduced from [178] by permission of The Royal Society of Chemistry.

BSA was driven by the EOF to concentrate at the depletion zone and 15 000-fold enhancement was achieved for 1 nM BSA in 1 mM PBS within 60 min, which is fourfold per second. This is lower that what is already reported for NMIs and the data were obtained in low-concentration buffer. It is known that enhancement factors drop massively with increasing the electrolyte concentration and we expect even lower EF if biological samples were used.

2.3.2.5 Other methods

Controlled etching with monitoring current through the capillary wall or alarm sound when enough current was conducted resulted in very small pore size, which leads to using the NMI for concentration on the enrichment or depletion side for both negative and positive compounds. An outstanding 10^9-fold concentration was achieved within 20 min using autostop HF-etching of fused silica capillary for 1 pM fluorescein in 1 mM Tris-HCl, pH 9.2 [182]. Unlabeled DNA was concentrated by 50-fold within 300 s using BGE of 80 mM MES-Tris (pH 6.18) with 0.8% HEC and UV detection. The dramatic drop in concentration enhancement by increasing BGE ionic strength demonstrates a common problem faced when applying these methods to biological samples. Although the method is efficient in concentrating wide range of analytes, special safety measures should be taken as the procedure includes using 30 μL of 40% HF for etching.

Arrayed multiwalled carbon nanotubes were used to concentrate biomolecules by up to 10^6-fold in 45 min [183]. The Parylene-multiwalled carbon nanotubes have controllable and highly dense charge on the surface, which facilitates high-concentration factors. EDL overlap can be achieved by increasing the applied voltage and selectively trap or release molecules based on charge or size, which demonstrates the size sieving and the electrostatic exclusion functions of the device.

2.3.3 Efforts for improvement

Stability of the depletion or concentration zones for as long as possible means increased enhancement factors. Louer et al. demonstrated the use of external hydrodynamic pressure to achieve concentration on the anodic or cathodic side of the NMI using the same device design and demonstrated stable ICP [184]. The 150-nm nanochannels were made in glass.

The ultimate goal is to have these devices incorporated into portable devices and minimize their power consumption needs. This means that devices can be left in remote areas for longer periods. It may include environmental analysis in the deep seas or desert or even searching for life on other planets. By removing the need for external power supply to drive the ICP, the energy can be saved to operate separation and detection. Electrodes with different reducibility were used in weak oxidizing solution to create electrochemical potential that is capable of producing ion depletion and enrichment zones near nanochannels without the need for external power supply [185]. Glass etching was used to create the fluidic structures including an array of 20 nanochannels, 200 nm deep. Pt electrode was used as anode and either Al or Fe as cathode to reach enhancement factors of fluorescein in 10 mM KCl of 40.2- and 27.1-fold, respectively, which indicates a relation between the enhancement factor and electrode material due to differences in the standard electrochemical potential. While fluorescein concentration was achieved within 20 s and lasted for few minutes, no enrichment was observed for the positively charged R6G.

As discussed above, ICP phenomena associated with NMI can provide astonishing enhancement factors up to 10^9-fold. The main problem, however, is their modest performance when handling biological samples due to high ionic strength. More effort in this area is required to maintain efficient concentration at high ionic strength by finding new materials that offer higher density surface charge, stability over wide range of pH, and well-defined and homogenous pore size.

3 Extraction

3.1 SPE

The sensitivity of CE can be enhanced by SPE to extract analytes prior to CE analysis, especially when large sample volumes should be concentrated. It can be performed in-line or on-line, with respect to the CE or microchip CE system. The effort to couple SPE with electrophoresis is thriving as evidenced by growing number of reviews on this topic alone [2, 11–13].

3.1.1 In-line SPE-CE

In in-line SPE-CE, a concentrator is synthesized or inserted (as a short column) directly into the inlet of the separation capillary. This means that extraction, enrichment, elution, and separation are carried out in the same capillary without further transfer of the eluting solution. In this way, the sample volume and organic solvents consumed for elution are minimized, and more importantly, automation of SPE-CE in commercial CE instruments can be realized.

3.1.1.1 Packed bed columns

The easiest way to create a packed bed is the "fritless" approach in which a large id section of capillary is packed with particles and connected to capillary with an id smaller than the particles. Tak et al. used this approach with 60-μm particles retained in a 2-mm bed (150 μm id capillary), sandwiched between 50 μm id separation capillaries, for the extraction of drugs of abuse for CE-MS [186]. Efficient elution was achieved by using 85% methanol in water acidified with acetic acid. Injecting 30 capillary volumes of sample (930 mbar for 60 min)

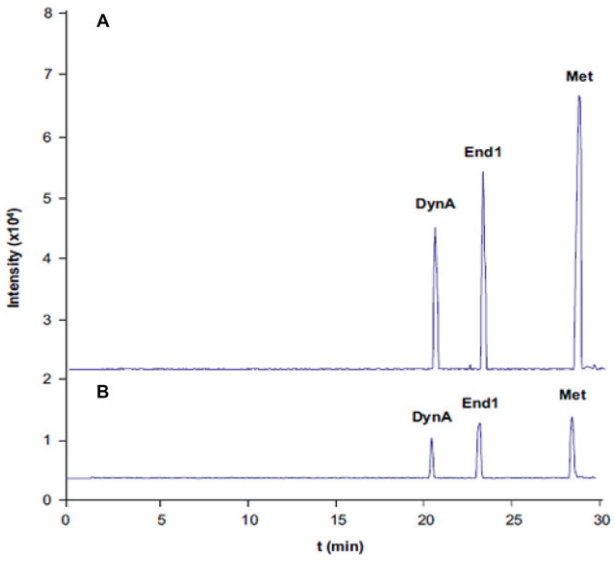

Figure 9. Sum of the extracted ion electropherograms of standard mixtures of dynorphin A, End1, and metenkephalin obtained by sheathless SPE-CE-MS loading: (a) 1.5 μL and (b) 8 μL of a 0.1 ng/mL standard mixture. Separations were performed by applying 50 mbar and a voltage of 30 kV. Reproduced from [189].

yielded SEFs between 2560 and 2930, with LODs between 0.22 and 24 pg/mL.

Maijo et al. used a mixed-mode phase for in-line SPE-CE-MS of four UV filters [187]. The sample was loaded at 930 mbar for 15 min, and the retained analytes eluted in 30 nL of ACN. A small plug of BGE (50 mbar for 200 s) was used to push the elution plug through the concentrator. SEFs of 3400–34 000-fold were obtained with LODs as low as 0.01 ng/mL. The method was applied to river water samples, however off-line SPE was required to achieve the low picogram per milliliter sensitivity required.

Jooß et al. prepared a "bead string design" SPE column in which a 4-mm section of 100 μm id capillary is filled with a string of 90 μm mixed-mode beads [188]. This design prevents clogging or formation of hollow spaces inside SPE column, which usually happens in conventional packed bed design. Capillary volumes (0.6–6) of sample were injected and eluted with a 35 nL plug of methanol/ammonia (95:5%, v/v). A recovery of 106% was achieved, and lower LODs (low nanomolar range) were achieved for 8-aminopyrene-1,3,6-trisulfonate (APTS)-labeled glycans, which corresponds to an enrichment factor of ≥800 compared to the normal hydrodynamic injection CE-MS. Later, the same group developed a micro-SPE cartridge for sheathless CE-MS employing a prototype porous-tip capillary for nano-ESI [189]. A 4-mm concentrator capillary (150 μm id) packed with 55–105 μm C18 particles was used for three opioid peptides; dynorphin A, End1, and metenkephalin. As shown in Fig. 9, when 8.5 μL sample was loaded, an SEF of 5000 was achieved (LOD 2 pg/mL); providing sensitivity that could not be achieved by sheathless CE-MS or sheath liquid SPE-CE-MS alone.

3.1.1.2 Monolithic columns

Monolithic columns are attractive for SPE-CE because they can be prepared frit-free in capillaries or microchip, however, this requires replacement of the entire capillary once the SPE column has reached the end of its life. Wu et al. prepared a poly(4-VP-co-EDGMA) monolith in a separate piece of capillary that was connected to the separation capillary by a Teflon tube [190]. The monolithic SPE column had good robustness (over a hundred injections) and high extraction efficiency. The SEF was 615–2222 folds with LODs of 1.3–3.3 ng/mL for a number of phenols. Zhai et al. used a similar approach in microchips in which a molecular imprinted monolith inside a capillary was embedded in a glass/PDMS microchip for on-line extraction and separation of auramine O [191]. The retained analytes were eluted with 20 μL methanol from which auramine O was electrokinetically injected. An enrichment of 12 was reported, with an LOD down to 2.5 μg/mL and this method was used for auramine O in shrimp meat purchased from local supermarket.

Nge et al. synthesized a butyl methacrylate monolith in a cyclic olefin copolymer microchip for the extraction and on-chip labeling of proteins and amino acids [192]. The protein loading capacity of the 2-mm monolith was 2 μg (30 pmol) of BSA. More importantly, the SPE-microchip design enabled further purification during elution due to the fact that the labeled analytes were more strongly retained on the monolith than the unattached fluorescent label. The SPE provided enrichment factor of between 6 and 11 folds. While LODs were not reported, linear relation between the eluted peak areas and concentrations of proteins demonstrated the potential for this to be quantitative.

3.1.1.3 Other approaches for SPE integration

The simplest method to construct an SPE column in-line is to coat a small portion of the separation capillary. Zhang et al. used an LED to photoinitiate the formation of a molecular imprinted SPE phase on the inner surface of a 3-mm section of capillary [193]. Enrichment factor up to 200 for epitestosterone, methyltestosterone, and testosterone was obtained compared to the injection without SPE.

Phillips et al. developed a chip-based SPE-CE system to isolate and determine six pro-inflammatory chemokines from infants' cerebrospinal fluids using reactive antibody fragments of antichemokine antibodies immobilized onto a 2-mm glass fiber disk [194]. The isolated analytes were labeled and eluted with acidic buffer to disrupt the complex releasing the chemokines for electrophoresis. The IA-SPE-CE showed good agreement with a commercial ELISA ($r^2 \geq 0.903$), with the developed method having tenfold superior sensitivity (LOD 0.5 pg/mL).

3.1.2 On-line SPE-CE

Unlike in-line SPE-CE, on-line SPE-CE has the SPE column coupled to CE system in an automated way, typically via an interface with flow-switching ability. Undoubtedly,

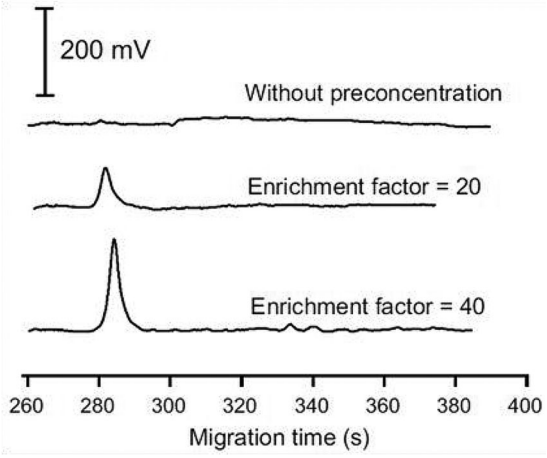

Figure 10. Analysis of a water sample taken from a wastewater treatment plan of a hospital in Hanoi, Vietnam. Reproduced from [195] with permission.

this approach permits relatively independent operation, as exemplified by Mai et al. involving automated on-line SPE using sequential injection manifold coupled with CE-C^4D [195]. For SPE (100 mg cartridge containing C18 particles), a second holding coil was included as a reservoir to hold eluted solution before it was delivered to the CE interface for hydrodynamic injection. Pharmaceutical samples (ibuprofen, diclofenac, naproxen, and bezafibrate) were loaded at 140 μL/s onto the cartridge, with the retained analytes eluted with 500 μL Tris/lactic acid/ACN (pH 8.0) solution. A preconcentration factor of 750 was achieved, with LOQs in the low nanomolar range. The method was successfully applied for the detection of ibuprofen from hospital waste water, which was barely detected without SPE. Electropherograms for the sample with and without SPE are shown in Fig. 10.

Polo-Luque et al. demonstrated another dimension of in-line SPE based on a piston inserted in the sample vial [196]. The extraction unit operated as a spin column to preconcentrate three nitrophenols, which was inserted into the sample vial. The subsequent elution and injection were performed in-line, placing the vial on the CE carousel. Good analyte sensitivity was achieved, with LODs ranged between 0.22 and 0.28 μg/L, making this a simple and interesting way of automating the SPE process for CE.

3.2 Liquid–liquid extraction (LLE)

LLE is an easy and simple sample-handling technique. Unlike SPE, LLE allows up-concentration from the sample solution directly into a receiving phase, rather than requiring a secondary elution step with a solvent. Moreover, no excessive pressure is required. In order to accommodate small sample volumes or reduce the amount of organic solvents required, a variety of miniaturized LLE methods, with or without a membrane as phase barrier, have been proposed and coupled directly to CE. Such methods include single-drop microextraction (SDME) [197, 198] and liquid-phase microextraction [199]. In order to avoid any band broadening due to sample overloading in CE, the injected sample volume in CE is usually limited to 1–2% of the total capillary volume. With the possibility of obtaining volume of acceptor extract in microliters or in quantities as small as a few nanoliter ranges, the in- and on-line coupling of miniaturized LLE with CE becomes more suitable.

In SDME, targeted analytes are extracted from a sample solution into an acceptor phase drop. After extraction, the drop is analyzed with an analytical instrument. Off-line coupling is normally used for LC and GC hyphenation while the hyphenation with CE can be performed either in the off-, at-, or on-line mode [200]. The development and feasibility of SDME as a pretreatment tool for CE was recently reviewed by Al Othman et al. [201]. The authors comprehensively describe basic principles, instrumentation, and modes of coupling in SDME-CE along with the recent developments and applications of SDME-CE in analyzing different sample matrices. Cheng et al. [202] demonstrated the possibility of in-line coupling of SDME with CE to analyze arsenic compounds in spiked tap water. Due to the hydrophilic nature of arsenic substances, a cationic carrier, namely aliquat 336, was added to the organic phase to promote the transfer of negatively charged arsenic species from sample into the acceptor drop hanging at the inlet of the capillary. Enrichment factors in the range of 390–1300 were achieved for targeted arsenic species with a 15-min extraction. In a fascinating combination, Park et al. [203] demonstrated the automated coupling of headspace SDME (HS-SDME) with LVSEP for phenolic compounds. The success combination of powerful sample pretreatment technique with LVSEP-CE has resulted in high sensitivity. The enrichment factor of phenolic compounds in red wine was 1900- to 3400-fold sensitivity.

Liquid-phase microextraction based on supported liquid membrane (SLM) has gained substantially popularity in the field of sample pretreatment due to its effective sample cleanup, low organic solvent usage, and cost effectiveness. The SLM consists of a porous polymeric material, which is impregnated with a water-immiscible organic solvent and adopted as a selective barrier between two aqueous solutions. Recently, Kubáň and Boček [204] published a detailed overview on the practicability of direct coupling of flat sheet based SLMs to CE, covering fundamental and instrumental aspects. Pantůčková and co-workers [205] proposed a simple device that enables direct in-line coupling of SLM extraction to a commercial CE system for rapid determination of selected basic drugs spiked in human urine and serum. The extraction setup was assembled in a sample vial and subsequently placed in an autosampler carousel of a commercial CE system. The position of the separation capillary injection end and high-voltage electrode in the CE instrument was precisely optimized to ensure efficient injection of sample. The SLM was discarded after each extraction eliminating sample carry over and tedious SLM regeneration steps. Schematic of SLM device for in-line coupling to a commercial CE

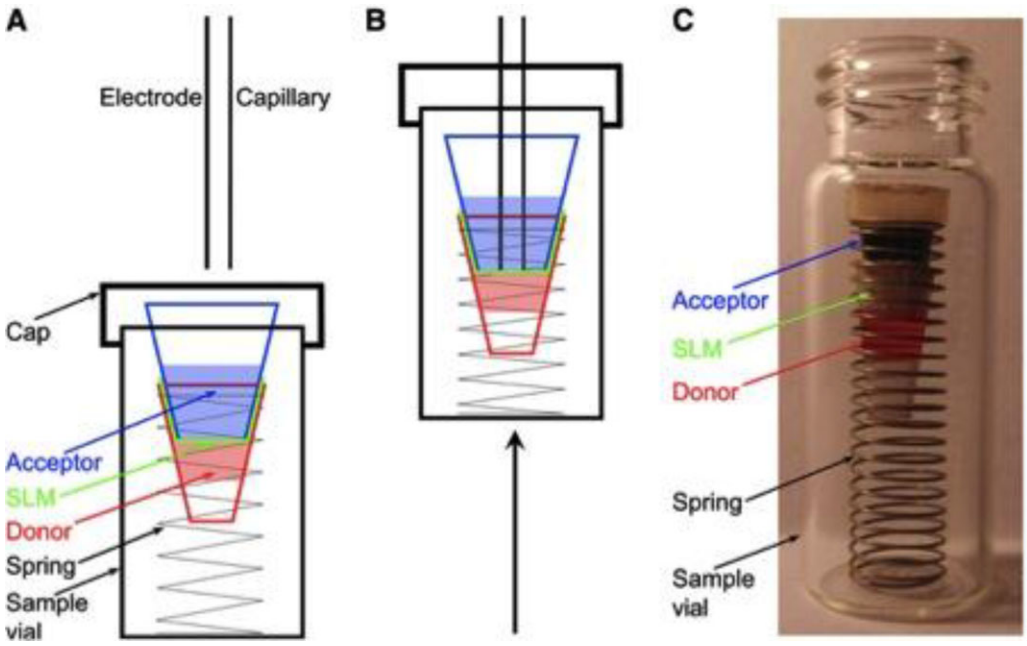

Figure 11. Sample pretreatment device for in-line coupling to a commercial CE instrument. (A) Sample vial before sample injection, (B) sample vial during injection of the pretreated sample (separation capillary and high-voltage electrode are in contact with SLM), and (C) a photograph of the sample vial with the assembled sample pretreatment device; the acceptor unit is partly hidden by the SLM. Reproduced from [205] with permission.

instrument is shown in Fig. 11. Similar approach with slight modification was adopted by the same research group for rapid determination of formate in undiluted blood samples [206]. Entire procedures, including SLM extraction, injection of extract, CE separation, and detection, were performed fully automatically.

LLE techniques based on the use of an electrical field as driving force are currently also receiving attention. The use of an electrical field allows better control of the extraction of charged species, and the methods tend to be faster than those of passive diffusion. Electroextraction is performed by applying an electric field to a two-phase liquid system consisting of an aqueous and an organic phase. Lindenburg et al. [207] demonstrated the feasibility of electroextraction as sample preconcentration step for fast and sensitive analysis of urine metabolite, in combination with LC or CZE. Urine metabolites present in the ethyl acetate were electroextracted into an aqueous acceptor phase by an electrodriving force. Note that no membrane is used as an organic/aqueous phase barrier in this case. Acylcarnitines along with more than 100 presumed metabolite peaks were successfully detected when final extract was analyzed with CZE-MS system.

Another alternative, termed "electromembrane extraction" (EME), is carried out by applying a voltage between an aqueous sample solution and the aqueous acceptor solution behind the organic solvent immobilized SLM. Payán et al. [208] described an in-line coupling of nano-EME procedure with CE system to monitor selected basic drug substances from 200 μL sample solution. A crack was made in the fused silica capillary and covered by heat-sealing a piece of hollow fiber membrane. SLM was formed by impregnating porous membrane with a drop of organic solvent. The electrical potential sustained over the SLM acted as the main driving force of the extraction. As the acceptor phase volume within the fused silica capillary in nano-EME was downscaled to approximately 8 nL, a 500-fold enrichment of loperamide within 5 min of extraction was achievable. A schematic of the nano-EME system and its in-line coupling with CE is shown in Fig. 12. On the other hand, several research groups have proposed new membrane materials as an alternative to SLM to further improve the durability of EME. See and coworkers demonstrated the use of a polymer inclusion membrane, a self-assembly homogenous thin-film polymeric membrane, in EME with off-line CE to determine inorganic anions [209] and herbicides [210] in water samples. The membrane was sandwiched between two PTFE blocks and the extraction was performed in a flow-through design, which is potentially to be on-line coupling with CE analysis. Kubáň and Boček [211] proposed a new micro-EME approach using a free liquid membrane as an alternative to SLM to extract basic drugs from undiluted biological samples. The extraction was carried out within a 1.0 mm id/1.6 mm od perfluoroalkoxy (PFA) tubing. The free liquid membrane consisted of 1.5 μL of 1-ethyl-2-nitrobenzene, which was used as a phase interface. The interface enabled selective electro-transport of basic drugs from 1.5 μL of a biological sample into a 1.5 μL acceptor solution in about 5 min at an extraction voltage of 100 V. After micro-EME, the acceptor phase within the perfluoroalkoxy tube was directly injected into CE and the LODs were <1 mg/mL for all examined matrices.

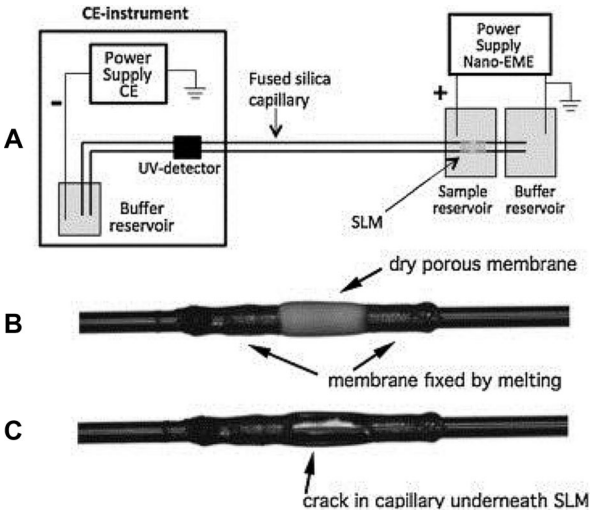

Figure 12. (A) Schematic illustration of the nano-EME system in nanoextraction mode and image of a 375 μm od fused silica capillary with crack and SLM, B) before and (C) after filling the pores with NPOE. Reproduced from [208] with permission.

4 Sequential stacking methods

4.1 Sequential stacking featuring sweeping

Using long EKI times, a significant portion of the sample ions can be injected into the capillary, however, the stacked peak is typically broad due to overloading the stacking mechanism and diffusion. Sweeping is an ideal second concentration mechanism to refocus and concentrate the overloaded analytes because the mechanism is complimentary to most other stacking mechanisms, and can thus be combined with FASI, dynamic pH junction, etc., to create a highly selective and powerful concentration approach.

4.1.1 Field-amplified injection–sweeping

Six papers combined FASI and sweeping, five of which used SDS as pseudostationary phase [212–216] and one used sodium taurodeoxycholate (STDC) [217]. Sensitivity enhancements between 30 and 900 were obtained after optimization and allowed the successful elucidation of homocysteine thiolactone in urine, ractopamine and dehydroxyractopamine in porcine meat, 5-nitroimidazole compounds in river and well water, DNA fragments in highly saline matrix, and DL-amino acids.

Tian et al. used FASI–sweeping with dendritic polyamidoamine generation 2.0 (PAMAM G 2.0) as the pseudophase for sweeping [215]. DNA and other sample ions were injected under negative polarity such that the co-ions traversed through the PAMAM G 2.0 zone, while the DNA fragment was swept by the dendrimer, thus serving to simultaneously purify and concentrate the DNA. An SDS micelle solution was hydrodynamically introduced into the capillary to complex with PAMAM G 2.0, releasing the DNA, which also induced a tITP zone. The developed approach obtained detection limit of 0.49 ng/mL, and SEFs of 30 and 3500 were obtained when compared with FASI and conventional hydrodynamic injection, respectively.

Polyethylene oxide (PEO)-based stacking and sweeping was proposed by Lin et al. for the simultaneous determination of nine pairs of DL-amino acids in CE [217]. The analytes were derivatized off-line with FMOC before detection. β-CD and STDC were used as chiral selector and pseudostationary phase, respectively. The capillary was filled with background solution containing Tris-borate, β-CD, and STDC before large plug of sample solution was hydrodynamically introduced. The vials were then replaced with BGE containing PEO, β-CD, and STDC micelles. The amino acids were swept by the anionic STDC micelles migrating through the sample zone and then stacked when encountering the viscous PEO BGE at the rear of the sample. PEO-stacking and sweeping with STDC micelles jointly affected the preconcentration of the analytes, further enhanced by the derivatization of the amino acids with FMOC. LODs in the range of 40–60 nM were attained.

4.1.2 Dynamic pH junction–sweeping

Hsu et al. used dynamic pH junction–sweeping for the determination of benzoic and sorbic acid [218]. The analytes were prepared in phosphate buffer at pH 3.0, while the tetraborate background solution had a pH value of 9.2. When voltage was applied, the hydroxide ions in the BGE migrated to the sample zone, increasing the pH of the sample plug. At high pH, benzoic and sorbic acid dissociated from neutral to anionic analytes, and halted abruptly at the front end of the sample zone. Simultaneously, the SDS micelles present in the BGE sweep the analytes into thin zone. The presence of PEO in the buffer also added to the stacking effect of the analytes. LODs of 8.2 and 6.1 nM for benzoic and sorbic acid were achieved, respectively, with an SEF of 900.

4.1.3 AFMC–sweeping

A novel method involving AFMC and sweeping to perform 2D heart-cutting CE in a single capillary was developed by Kukusamude et al. [219] for the separation of neutral and cationic analytes. After a long plug of the sample was introduced into the capillary, the vials were replaced with CZE electrolytes and then voltage at positive polarity was applied. Stacked cationic analytes migrated toward the detector and were separated via CZE. Continuous application of voltage caused the further migration of the cations out of the capillary. Only neutral analytes were left inside the capillary for separation. Both ends of the capillary were then replaced with low-pH MEKC electrolyte containing SDS micelles for sweeping and separation of the neutral analytes. SEFs from 15 to 100 for two artificial mixtures of cations and neutral

compounds were achieved. The developed method was successfully applied to river water sample spiked with the model analytes.

4.1.4 Field-amplified injection–MSS

Rabanes et al. [220] recently combined FASI and MSS, the mechanism of which is shown in Fig. 13, for the concentration of cations. Here, the SDS micelles and analytes under FASI conditions migrate into an organic solvent where the micelles collapse and release the cationic analytes. The released analytes have a reversed electrophoretic velocity, which results in the cations focusing around the organic solvent/sample boundary. FASI allowed the introduction of more analytes into the capillary because of the difference in conductivities of the BGS and sample solution zones. Improvements in SEF of three orders of magnitude were achieved by this approach. This was modified by Tubaon et al. [221] for the analysis of anionic sulfonamides in fortified river water samples using the cationic surfactant, CTAB, for analyte transport. LOQs in the range of 0.01–0.03 μg/mL were achieved for three sulfonamide compounds. Kukusamude et al. used this for herbicides after cloud-point sample preparation in milk [222] and with CE-MS by Wuethrich et al. for the racemic drug chlorpheniramine maleate [33].

4.2 Electrokinetic supercharging

Electrokinetic supercharging (EKS) is a two-step stacking that employs tITP to preconcentrate analytes after a significantly long FASI [223]. Consequently, EKS is able to provide massive improvement in sample enrichment than sole FASI or ITP [2, 224–227]. Following their original contribution for increasing sample volume and electrode configuration, Hirokawa and co-workers described a similar system to that published in 2009 for larger molecules, specifically dsDNA fragments [228]. The authors aimed to maintain the effective field strength over large space inside the sample vial, which was achieved by increasing the distance between the electrode and capillary inlet tip from 3.6 mm to 16 and 24 mm, with the latter requiring the use of a platinum ring

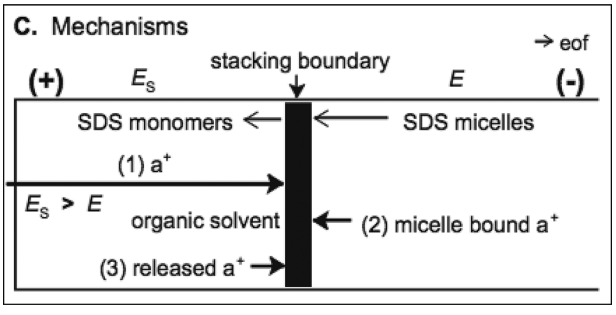

Figure 13. Mechanism for FASI and MSS in CE, which has been explained in the text. Reproduced from [220] with permission.

electrode that significantly increased the area of effective electric field inside the sample vial (Fig. 14). It is worth noting that increasing the electrode–capillary tip distance from 3.6 to 16 mm using the hollow electrode design found in the Agilent instrument resulted in twofold enhancement in detection sensitivity, however, the LODs obtained with the Pt-ring electrode were 20-fold lower than the original hollow electrode. After electrolyte optimization, the LOD of the EKS system was 8 pg/mL, 10 000-fold lower than without EKS.

In the above-mentioned work, a valuable observation was reported and studied in a following research article [229]. It was found that the peak area of DNA fragments decreased with increasing the injection voltage from 2 to 10 kV when the electrode was positioned 16 mm from the capillary. This phenomenon has been attributed to the aggregation of DNA fragments and has been already confirmed by Song and Maestre during the analysis of DNA with high molecular weight several years ago [230]. However, the Hirokawa group postulated that another contributor for the decrease in peak area is the possible cleavage of the DNA due to high electric field strength especially at the area between the electrode and capillary inlet tip. The authors performed a highly comparative study that was supported by computer simulations. They varied the electrode distance from 2 to 40 mm and varied the injection voltage from 2 to 20 kV. The authors noticed that at a distance of 4 mm, an injection voltage of 20 kV resulted in about 20% damage of DNA when compared to 2 kV. This damage was increased to 50% when the distance was increased to 10 mm with an injection voltage of 1 kV, and at 40 mm, significant damage could be found when injecting at 5 kV. Although the mechanism of DNA fragmentation and/or cleavage in this work is not clearly presented, yet the significance of this study lies in the fact that it reveals the limitations and highlights certain considerations to be undertaken during EKI of DNA under field-amplified conditions.

Since long FASI is usually employed in EKS, the movement of stacking boundary is a major obstacle for the EKI step. This movement will not only deteriorate the efficiency of stacking step, but it will also jeopardize the room available for the subsequent ITP stacking and the final separation step. This limitation can be addressed by application of a hydrodynamic flow [231–235]. Chung's group has applied CF-EKS in the constant voltage mode for the analysis of catecholamines [30]. The authors applied a hydrodynamic CF during the EKI step in order to balance the movement of the stacking boundary. They were able to inject their analytes at 25 kV for a significantly long time (30 min) with the aid of a counterpressure of 1.3 psi. Additionally, they compared constant voltage and constant current, with constant voltage providing more efficient separation and preconcentration than the constant current due to more regulated and defined voltages over the different sections of the capillary. The LODs of catecholamines analyzed by the CF-EKS system were down to 1.2 nM and the enrichments in the UV detection sensitivity were up to 50 000-fold.

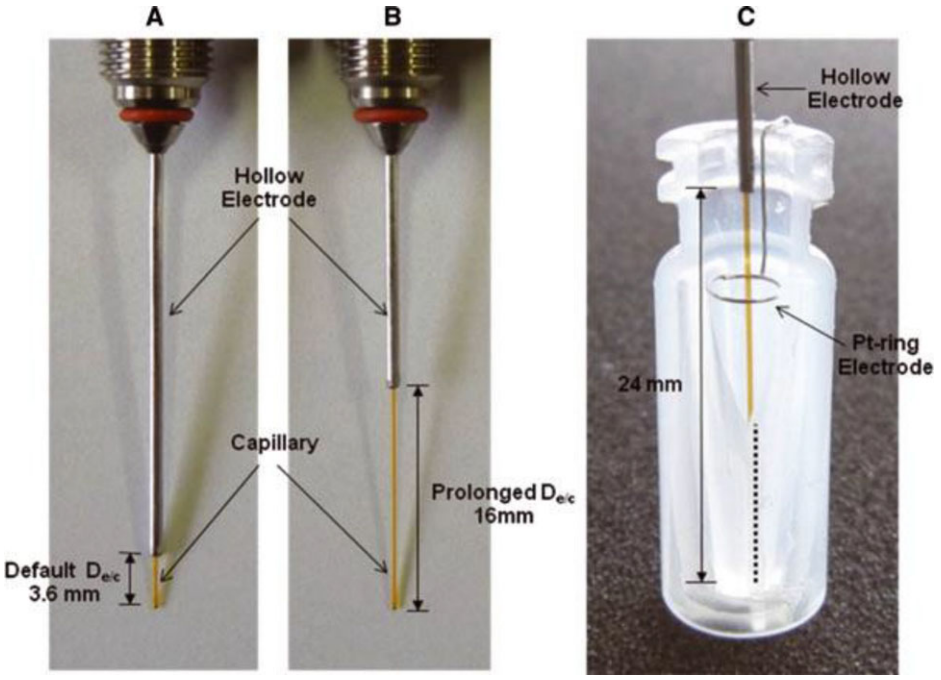

Figure 14. Images of electrode configuration: The hollow electrode with (A) the default electrode–capillary distance of 3.6 mm and (B) prolonged distance of 16 mm; (C) the Pt-ring electrode fixed in the sample vial that is positioned around inlet of the capillary end. Reproduced from [228] with permission.

4.3 Interfacing multidimensional separations

The peak capacity and selectivity achievable by traditional 1D separation techniques is not sufficient to adequately resolve complex samples where a wide range of analytes with a variety of different properties are present. The coupling of orthogonal techniques of fundamentally different separation mechanisms can be used to enhance peak capacity and therefore resolving power [236]. In the field of electrophoresis, this is nothing new, as it has been the basis for 2DE that was the cornerstone of proteomics for more than two decades. It is the extension of this increase in resolving power to nonproteins that has gained much recent interest [219, 237–241].

The coupling of ITP with CE in a column-coupled approach is well established, with a highly successful commercially available instrument to perform this. Over the past 2 years, it has been used for glyphosate in drinking water [242], bromate in drinking water [243], and tyramine, 2-phenylethylamine, and histamine in red wines [244].

A column coupled capillary ITP-CZE was used for determination of quinine in human urine [245]. The ITP step allows larger sample volume to be injected (30 μL) giving an LOD of 8.6 ng/mL. The authors then studied cITP-CZE-LIF for quantitative determination of quinine [246]. When even this provides insufficient performance, it is possible to add a third dimension: ITP-ITP-CZE [247]. The first ITP was for preseparation and the second ITP step served to refine this further and remove the remaining matrix constituents prior to CZE analysis. The LOD of phthalic acid in reference sample was 150 ppb, while it was 400 ppb for urine samples with repeatability of peak area for six runs <2% and migration times of phthalic acid peaks for six runs was <1% using UV detector.

Wu et al. performed a 2D separation using IEF followed by tITP/CZE for on-chip labeling for protein determination in infant milk formula using UV detection [248]. The results show a 60-fold enrichment of the isolated protein fractions. The authors then used the method for analysis of soybean protein in dairy products [249]. The use of IEF at p*I* range of 5.5–7.0 allows the soybean proteins to be isolated into fractions and the fractions of proteins then transferred into the embedded capillary for tITP-CZE for preconcentration separation and detection using UV detector. This method allows detection of soybean protein as low as 0.1% in total dairy proteins. The enhancement factor obtained using 2D microchip-CE device compared to IEF-CZE was 20 times

With substantially orthogonal mechanism compared to most chromatographic approaches and considerably shorter analysis time, LC-CE is theoretically an ideal combination. However, coupling the two dimensions is challenging, given there is a mismatch of volume, where the typical solution is an extremely large splitting of the LC effluent to accommodate the typical CE injection volume [250]. As a result, interfacing CE as the second dimension places a great burden on detection and urges utilization of preconcentration techniques. An example of this appears in the study by Česla et al., where to compensate for approximately 20-fold dilution of the sample in the LC effluent in off-line LC-MEKC, in-capillary sweeping by SDS micelles was utilized to preconcentrate and separate natural antioxidants in red wine [237]. In a simple and interesting way to perform LC-CE, Wang et al. [101] utilized a short SPE column in the front of the capillary and multistep elution prior to tITP and sheathless CE-MS to improve the coverage of peptide analysis from protein digests. A 1-mm concentrator was prepared by creating a frit at one end of a 100 μm id/360 μm od capillary that was packed with 5 μm C8 particles.

Tryptic digests were first loaded onto the SPE column, and then sequentially eluted with a 50 mM ammonium acetate buffer with increasing amounts of methanol and isopropanol (10–10, 20–20, 30–30, 40–40, 48–48 v/v) with each eluted fraction separated by tITP. From comparative analysis of SPME-tITP-CE with direct injection CE, the SPME-tITP step improved comprehensiveness and sensitivity, as evidenced by the improved S/N for all peptide precursor intensities.

Despite the few already published reports on comprehensive LC-CE, there are no reports on using stacking/sweeping approaches to improve analyte transfer and there is a substantial need for novel interfacing and sensitivity improvement approaches to allow full use of the potentials of such systems.

5 Concluding remarks

On-line concentration is one of the most widespread areas of interest within the field of electrophoresis and it is likely to remain a focus of the field in the endeavor to create sensitive, universal systems for a range of applications. Key areas that are being addressed over the past 2 years are in efforts to deal with matrix effects, and to minimize those, as well as to make simpler, more robust methods, particularly for implementation in portable devices where the aim is to reduce and minimize the need for complex manual handling. This aspect will receive more attention as the push toward complete sample-in/answer-out system continues. Importantly, there is no approach that is universal—selection of the right approach for the right application remains a challenge and is perhaps the hardest part of the process.

The Australian Research Council is thanked for funding and provision of a QEII Fellowship to MCB (DP0984745) and a Future Fellowship to JPQ (FT100100213). AAA Acknowledges Al-Zaytoonah University of Jordan for financial support. PP would like to thank the Thailand Research Fund through the Royal Golden Jubilee Ph.D. Program, The Higher Education Commission and Mahidol University (grant no. PHD/0306/2551). HHS thanks the Swiss National Science Foundation through Advanced Mobility (grant no. P300P2-147771).

The authors have declared no conflict of interest.

6 References

[1] Breadmore, M. C., *J. Chromatogr. A* 2012, *1221*, 42–55.

[2] Breadmore, M. C., Shallan, A. I., Rabanes, H. R., Gstoettenmayr, D., Abdul Keyon, A. S., Gaspar, A., Dawod, M., Quirino, J. P., *Electrophoresis* 2013, *34*, 29–54.

[3] Malá, Z., Křivánková, L., Gebauer, P., Boček, P., *Electrophoresis* 2007, *28*, 243–253.

[4] Malá, Z., Šlampová, A., Gebauer, P., Boček, P., *Electrophoresis* 2009, *30*, 215–229.

[5] Aranas, A. T., Guidote, A. M. Jr., Quirino, J. P., *Anal. Bioanal. Chem.* 2009, *394*, 175–185.

[6] Malá, Z., Gebauer, P., Boček, P., *Electrophoresis* 2011, *32*, 116–126.

[7] Kazarian, A. A., Hilder, E. F., Breadmore, M. C., *J. Sep. Sci.* 2011, *34*, 2800–2821.

[8] Šlampová, A., Malá, Z., Pantůčková, P., Gebauer, P., Boček, P., *Electrophoresis* 2013, *34*, 3–18.

[9] Ross, D., Locascio, L. E., *Anal. Chem.* 2002, *74*, 2556–2564.

[10] Meighan, M. M., Staton, S. J., Hayes, M. A., *Electrophoresis* 2009, *30*, 852–865.

[11] Ramautar, R., Somsen, G. W., de Jong, G. J., *Electrophoresis* 2014, *35*, 128–137.

[12] Ramautar, R., Somsen, G. W., De Jong, G. J., *Electrophoresis* 2010, *31*, 44–54.

[13] Giordano, B. C., Burgi, D. S., Hart, S. J., Terray, A., *Anal. Chim. Acta* 2012, *718*, 11–24.

[14] Wen, Y., Li, J., Ma, J., Chen, L., *Electrophoresis* 2012, *33*, 2933–2952.

[15] Sánchez-Hernández, L., Castro-Puyana, M., Marina, M. L., Crego, A. L., *Electrophoresis* 2012, *33*, 228–242.

[16] Kitagawa, F., Otsuka, K., *J. Chromatogr. A* 2014, *1335*, 43–60.

[17] Chiu, T. C., *Anal. Bioanal. Chem.* 2013, *405*, 7919–7930.

[18] Chen, Y., Lü, W., Chen, X., Teng, M., *Cent. Eur. J. Chem.* 2012, *10*, 611–638.

[19] Breadmore, M. C., Sänger-Van De Griend, C. E., *LCGC N. Am.* 2014, *32*, 174–186.

[20] Dziomba, S., Biernacki, M., Oledzka, I., Skrzydlewska, E., Baczek, T., Kowalski, P., *Talanta* 2014, *125*, 1–6.

[21] Ono, K., Kaneda, S., Fujii, T., *Electrophoresis* 2013, *34*, 903–910.

[22] Deng, D., Deng, H., Zhang, L., Su, Y., *J. Chromatogr. Sci.* 2014, *52*, 357–362.

[23] Cheng, H., Han, C., Xu, Z., Liu, J., Wang, Y., *Food. Anal. Meth.* 2014, *7*, 2153–2162.

[24] Cai, C., Cheng, H., Wang, Y., *Anal. Meth.* 2014, *6*, 2767–2773.

[25] Cai, C., Cheng, H., Wang, Y., Yang, M., Yang, Y., *Anal. Meth.* 2013, *5*, 4978–4983.

[26] Zinellu, A., Sotgia, S., Deiana, L., Carru, C., in: Volpi, N., Maccari, F. (Eds.), *Methods in Molecular Biology* 2013, pp. 131–138.

[27] Bacaloni, A., Insogna, S., Sancini, A., Ciarrocca, M., Sinibaldi, F., *Biomed. Chromatogr.* 2013, *27*, 987–993.

[28] Zinellu, A., Sotgia, S., Deiana, L., Carru, C., *Methods in Mol. Biol.* 2013, *984*, 131–138.

[29] Ito, E., Nakajima, K., Waki, H., Miseki, K., Shimada, T., Sato, T. A., Kakehi, K., Suzuki, M., Taniguchi, N., Suzuki, A., *Anal. Chem.* 2013, *85*, 7859–7865.

[30] Kwon, J. Y., Chang, S. B., Jang, Y. O., Dawod, M., Chung, D. S., *J. Sep. Sci.* 2013, *36*, 1973–1979.

[31] de la Ossa, M. T. F., Torre, M., García-Ruiz, C., *Anal. Chim. Acta* 2012, *745*, 149–155.

[32] Guo, Y., Meng, L., Zhang, Y., Tang, W., Zhang, W., Xia, Y., Ban, F., Wu, N., Zhang, S., *J. Chromatogr. B* 2013, *942-943*, 151–157.

[33] Wuethrich, A., Haddad, P. R., Quirino, J. P., *Chirality* 2013, *26*, 734–738.

[34] Dziomba, S., Kowalski, P., Słomińska, A., Baczek, T., *Anal. Chim. Acta* 2014, *811*, 88–93.

[35] Us, M. F., Alshana, U., Lubbad, I., Göğer, N. G., Ertaş, N., *Electrophoresis* 2013, *34*, 854–861.

[36] Alshana, U., Göğer, N. G., Ertaş, N., *J. Sep. Sci.* 2012, *35*, 2114–2121.

[37] Liang, T. T., Lv, Z. H., Jiang, T. F., Wang, Y. H., *Electrophoresis* 2013, *34*, 345–352.

[38] Quirino, J. P., *J. Chromatogr. A* 2013, *1299*, 131–135.

[39] Chen, Z., Lin, Z., Zhang, L., Cai, Y., *Analyst* 2012, *137*, 1723–1729.

[40] Fan, L. Y., He, T., Tang, Y. Y., Zhang, W., Song, C. J., Zhao, X., Zhao, X. Y., Cao, C. X., *J. Forensic Sci.* 2012, *57*, 813–819.

[41] Cheng, Y. C., Wang, C. C., Chen, Y. L., Wu, S. M., *Electrophoresis* 2012, *33*, 1443–1448.

[42] Lee, I. S. L., Boyce, M. C., Breadmore, M. C., *Food Chem.* 2012, *133*, 205–211.

[43] Knob, R., Maier, V., Petr, J., Ranc, V., Ševčík, J., *Electrophoresis* 2012, *33*, 2159–2166.

[44] Li, P., Hu, B., Li, X., *J. Chromatogr. A* 2012, *1247*, 49–56.

[45] Quesada-Molina, C., del Olmo-Iruela, M., Garcia-Campana, A. M., *Anal. Meth.* 2012, *4*, 2341–2347.

[46] Wang, C. C., Chen, J. L., Chen, Y. L., Cheng, H. L., Wu, S. M., *Anal. Chim. Acta* 2012, *744*, 99–104.

[47] Ho, Y. H., Wang, C. C., Hsiao, Y. T., Ko, W. K., Wu, S. M., *J. Chromatogr. A* 2013, *1295*, 136–141.

[48] Lin, Y. Y., Wang, C. C., Ho, Y. H., Chen, C. S., Wu, S. M., *Anal. Bioanal. Chem.* 2013, *405*, 259–266.

[49] Tůma, P., *J. Chromatogr. A* 2014, *1345*, 207–211.

[50] Qi, S., Zhang, H., Zhu, Q., Chen, H., Dong, Y., Zhou, L., Ren, C., Chen, X., *Anal. Meth.* 2014, *6*, 1219–1226.

[51] Kawai, T., Ueda, M., Fukushima, Y., Sueyoshi, K., Kitagawa, F., Otsuka, K., *Electrophoresis* 2013, *34*, 2303–2310.

[52] Tůma, P., Šustková-Fišerová, M., Opekar, F., Pavlíček, V., Málková, K., *J. Chromatogr. A* 2013, *1303*, 94–99.

[53] Shen, C. C., Tseng, W. L., Hsieh, M. M., *J. Chromatogr. A* 2012, *1220*, 162–168.

[54] Maijó, I., Borrull, F., Aguilar, C., Calull, M., *Electrophoresis* 2013, *34*, 363–373.

[55] Duan, J., He, M., Hu, B., *J. Chromatogr. A* 2012, *1268*, 173–179.

[56] Fukushima, E., Yagi, Y., Yamamoto, S., Nakatani, Y., Kakehi, K., Hayakawa, T., Suzuki, S., *J. Chromatogr. A* 2012, *1246*, 84–89.

[57] Yamamoto, S., Nakatani, Y., Suzuki, S., *Anal. Sci.* 2013, *29*, 831–835.

[58] Kawai, T., Ito, J., Sueyoshi, K., Kitagawa, F., Otsuka, K., *J. Chromatogr. A* 2012, *1267*, 65–73.

[59] Kawai, T., Koino, H., Sueyoshi, K., Kitagawa, F., Otsuka, K., *J. Chromatogr. A* 2012, *1246*, 28–34.

[60] Li, J., Huang, Y., Huang, L., Ye, L., Zhou, Z., Xiang, G., Xu, L., *J. Pharm. Biomed. Anal.* 2012, *70*, 26–31.

[61] Zhu, J., Tian, S., Zhou, Y., Chen, X., *Asian J. Chem.* 2012, *24*, 3671–3674.

[62] Rang, Y., Zhang, W., Chen, Z., *Anal. Lett.* 2013, *46*, 2503–2513.

[63] Yi, L. X., Chen, G. H., Fang, R., Zhang, L., Shao, Y. X., Chen, P., Tao, X. X., *Electrophoresis* 2013, *34*, 1304–1311.

[64] Bahga, S. S., Santiago, J. G., *Analyst* 2013, *138*, 735–754.

[65] Smejkal, P., Bottenus, D., Breadmore, M. C., Guijt, R. M., Ivory, C. F., Foret, F., Macka, M., *Electrophoresis* 2013, *34*, 1493–1509.

[66] Khurana, T. K., Santiago, J. G., *Anal. Chem.* 2008, *80*, 6300–6307.

[67] Bercovici, M., Han, C. M., Liao, J. C., Santiago, J. G., *Proc. Natl. Acad. Sci. USA* 2012, *109*, 11127–11132.

[68] Garcia-Schwarz, G., Santiago, J. G., *Anal. Chem.* 2012, *84*, 6366–6369.

[69] Bahga, S. S., Han, C. M., Santiago, J. G., *Analyst* 2013, *138*, 87–90.

[70] Eid, C., Garcia-Schwarz, G., Santiago, J. G., *Analyst* 2013, *138*, 3117–3120.

[71] Garcia-Schwarz, G., Santiago, J. G., *Angew. Chem.* 2013, *52*, 11534–11537.

[72] Karsenty, M., Rubin, S., Bercovici, M., *Anal. Chem.* 2014, *86*, 3028–3036.

[73] Schoch, R. B., Ronaghi, M., Santiago, J. G., *Lab Chip* 2009, *9*, 2145–2152.

[74] Persat, A., Chivukula, R. R., Mendell, J. T., Santiago, J. G., *Anal. Chem.* 2010, *82*, 9631–9635.

[75] Persat, A., Marshall, L. A., Santiago, J. G., *Anal. Chem.* 2009, *81*, 9507–9511.

[76] Persat, A., Santiago, J. G., *Anal. Chem.* 2011, *83*, 2310–2316.

[77] Marshall, L. A., Wu, L. L., Babikian, S., Bachman, M., Santiago, J. G., *Anal. Chem.* 2012, *84*, 9640–9645.

[78] Marshall, L. A., Rogacs, A., Meinhart, C. D., Santiago, J. G., *J. Chromatogr. A* 2014, *1331*, 139–142.

[79] Shintaku, H., Nishikii, H., Marshall, L. A., Kotera, H., Santiago, J. G., *Anal. Chem.* 2014, *86*, 1953–1957.

[80] Rogacs, A., Qu, Y., Santiago, J. G., *Anal. Chem.* 2012, *84*, 5858–5863.

[81] Strychalski, E. A., Konek, C., Butts, E. L., Vallone, P. M., Henry, A. C., Ross, D., *Electrophoresis* 2013, *34*, 2522–2530.

[82] Prest, J. E., Baldock, S. J., Fielden, P. R., Goddard, N. J., Goodacre, R., O'Connor, R., Treves Brown, B. J., *J. Chromatogr. B* 2012, *903*, 53–59.

[83] Oukacine, F., Quirino, J. P., Destoumieux-Garzon, D., Cottet, H., *J. Chromatogr. A* 2012, *1268*, 180–184.

[84] Oukacine, F., Quirino, J. P., Garrelly, L., Romestand, B., Zou, T., Cottet, H., *Anal. Chem.* 2011, *83*, 4949–4954.

[85] Phung, S. C., Nai, Y. H., Powell, S. M., Macka, M., Breadmore, M. C., *Electrophoresis* 2013, *34*, 1657–1662.

[86] Saito, S., Maeda, T., Nakazumi, H., Colyer, C. L., *Anal. Sci.* 2013, *29*, 157–159.

[87] Jastrzębska, A., *Eur. Food. Res. Tech.* 2012, *235*, 563–572.

[88] Jastrzebska, A., Piasta, A., Szlyk, E., *Food Addit. Contam. A Chem. Anal. Control Expo. Risk Assess.* 2014, *31*, 83–92.

[89] Zgola-Grześkowiak, A., Grześkowiak, T., *Int. J. Food. Prop.* 2012, *15*, 628–637.

[90] Jarolimova, Z., Lubal, P., Kanicky, V., *Talanta* 2012, *98*, 49–53.

[91] Smejkal, P., Breadmore, M. C., Guijt, R. M., Grym, J., Foret, F., Bek, F., Macka, M., *Anal. Chim. Acta* 2012, *755*, 115–120.

[92] Smejkal, P., Breadmore, M. C., Guijt, R. M., Foret, F., Bek, F., Macka, M., *Anal. Chim. Acta* 2013, *803*, 135–142.

[93] Prest, J. E., Fielden, P. R., Qi, Y., *J. Chromatogr. A* 2012, *1260*, 239–243.

[94] Vio, L., Cretier, G., Chartier, F., Geertsen, V., Gourgiotis, A., Isnard, H., Rocca, J. L., *Talanta* 2012, *99*, 586–593.

[95] Taglia, V., *J. Chromatogr.* 1973, *79*, 380–382.

[96] Taglia, V., Lederer, M., *J. Chromatogr.* 1973, *77*, 467–471.

[97] Abelev, G. I., Karamova, E. R., *Anal. Biochem.* 1984, *142*, 437–444.

[98] Moghadam, B. Y., Connelly, K. T., Posner, J. D., *Anal. Chem.* 2014, *86*, 5829–5837.

[99] Shallan, A. I., Smejkal, P., Corban, M., Guijt, R. M., Breadmore, M. C., *Anal. Chem.* 2014, *86*, 3124–3130.

[100] Huang, S. W., Tzeng, H. F., *Electrophoresis* 2012, *33*, 536–542.

[101] Wang, Y., Fonslow, B. R., Wong, C. C. L., Nakorchevsky, A., Yates Iii, J. R., *Anal. Chem.* 2012, *84*, 8505–8513.

[102] Honegr, J., Pospisilova, M., *J. Sep. Sci.* 2013, *36*, 729–735.

[103] Heemskerk, A. A., Wuhrer, M., Busnel, J. M., Koeleman, C. A., Selman, M. H., Vidarsson, G., Kapur, R., Schoenmaker, B., Derks, R. J., Deelder, A. M., Mayboroda, O. A., *Electrophoresis* 2013, *34*, 383–387.

[104] Ren, H., Liu, X., Jiang, S., *J. Pharm. Biomed. Anal.* 2013, *78-79*, 100–104.

[105] Matczuk, M., Foteeva, L. S., Jarosz, M., Galanski, M., Keppler, B. K., Hirokawa, T., Timerbaev, A. R., *J. Chromatogr. A* 2014, *1345*, 212–218.

[106] Shihabi, Z. K., *Electrophoresis* 2000, *21*, 2872–2878.

[107] Shihabi, Z. K., *Electrophoresis* 2002, *23*, 1612–1617.

[108] Shihabi, Z. K., *J. Chromatogr. A* 1993, *652*, 471–475.

[109] Dziomba, S., Kowalski, P., Slominska, A., Baczek, T., *Anal. Chim. Acta* 2014, *811*, 88–93.

[110] Quist, J., Vulto, P., van der Linden, H., Hankemeier, T., *Anal. Chem.* 2012, *84*, 9065–9071.

[111] Shackman, J. G., Ross, D., *Electrophoresis* 2007, *28*, 556–571.

[112] Fosdick, S. E., Knust, K. N., Scida, K., Crooks, R. M., *Angew. Chem.* 2013, *52*, 10438–10456.

[113] Anand, R. K., Sheridan, E., Hlushkou, D., Tallarek, U., Crooks, R. M., *Lab Chip* 2011, *11*, 518–527.

[114] Anand, R. K., Sheridan, E., Knust, K. N., Crooks, R. M., *Anal. Chem.* 2011, *83*, 2351–2358.

[115] Perdue, R. K., Laws, D. R., Hlushkou, D., Tallarek, U., Crooks, R. M., *Anal. Chem.* 2009, *81*, 10149–10155.

[116] Knust, K. N., Sheridan, E., Anand, R. K., Crooks, R. M., *Lab Chip* 2012, *12*, 4107–4114.

[117] Scida, K., Sheridan, E., Crooks, R. M., *Lab Chip* 2013, *13*, 2292–2299.

[118] Cao, Z., Yobas, L., *Electrophoresis* 2013, *34*, 1991–1997.

[119] Shameli, S. M., Glawdel, T., Fernand, V. E., Ren, C. L., *Electrophoresis* 2012, *33*, 2703–2710.

[120] Han, T., Park, S., Jeon, T.-J., Kim, S. M., *Microsyst. Technol.* 2014. DOI 10.1007/s00542-014-2208-6

[121] Trickett, C. A., Henderson, R. D., Guijt, R. M., Breadmore, M. C., *Electrophoresis* 2012, *33*, 3254–3258.

[122] Ross, D., Romantseva, E. F., *Anal. Chem.* 2009, *81*, 7326–7335.

[123] Sikorsky, A. A., Fourkas, J. T., Ross, D., *Anal. Chem.* 2014, *86*, 3625–3632.

[124] Aebersold, R., Morrison, H. D., *J. Chromatogr. A* 1990, *516*, 79–88.

[125] Britz-McKibbin, P., Bebault, G. M., Chen, D. D., *Anal. Chem.* 2000, *72*, 1729–1735.

[126] Fan, Y., Li, S., Fan, L., Cao, C., *Talanta* 2012, *95*, 42–49.

[127] Yang, Q., Fan, L. Y., Huang, S. S., Zhang, W., Cao, C. X., *Electrophoresis* 2011, *32*, 1015–1024.

[128] Zhang, H., Zhang, W., Zhang, Z., Shi, Z., Liu, W., *J. Liq. Chromatogr. Relat. Technol.* 2014, *37*, 1145–1162.

[129] Tang, W., Ge, S., Gao, F., Wang, G., Wang, Q., He, P., Fang, Y., *Electrophoresis* 2013, *34*, 2041–2048.

[130] Hsieh, B. C., Chen, R. L. C., Tsai, T., *J. Sep. Sci.* 2013, *36*, 803–808.

[131] Acosta, G., Arce, S., Ortega, C., Martínez, L. D., Gomez, M. R., *Curr. Anal. Chem.* 2014, *10*, 197–204.

[132] Zhu, G., Sun, L., Yan, X., Dovichi, N. J., *Anal. Chem.* 2014, *86*, 6331–6336.

[133] Terabe, S., Otsuka, K., Ando, T., *Anal. Chem.* 1985, *57*, 834–841.

[134] Terabe, S., Otsuka, K., Ichikawa, K., Tsuchiya, A. Ando, T., *Anal. Chem.* 1984, *56*, 111–113.

[135] Quirino, J. P., Terabe, S., *Science* 1998, *282*, 465–468.

[136] Quirino, J. P., Terabe, S., *J. High Resol. Chromatogr.* 1999, *22*, 367–372.

[137] Quirino, J. P., Haddad, P. R., *Anal. Chem.* 2008, *80*, 6824–6829.

[138] Quirino, J. P., *J. Chromatogr. A* 2008, *1214*, 171–177.

[139] Quirino, J. P., *J. Chromatogr. A* 2009, *1216*, 294–299.

[140] Dziomba, S., Kowalski, P., Baogonekczek, T., *J. Chromatogr. A* 2012, *1267*, 224–230.

[141] Michalska, K., Cielecka-Piontek, J., Pajchel, G., Tyski, S., *J. Chromatogr. A* 2013, *1282*, 153–160.

[142] Fang, R., Chen, G. H., Yi, L. X., Shao, Y. X., Zhang, L., Cai, Q. H., Xiao, J., *Food Chem.* 2014, *145*, 41–48.

[143] Wang, C. C., Cheng, S. F., Cheng, H. L., Chen, Y. L., *Anal. Bioanal. Chem.* 2013, *405*, 1969–1976.

[144] Wang, Q., Qiu, H., Han, H., Liu, X., Jiang, S., *J. Sep. Sci.* 2012, *35*, 589–595.

[145] Hernández-Mesa, M., Cruces-Blanco, C., García-Campaña, A. M., *J. Sep. Sci.* 2013, *36*, 3050–3058.

[146] Rabanes, H. R., Quirino, J. P., *Electrophoresis* 2013, *34*, 1319–1326.

[147] Quirino, J. P., Terabe, S., Bocek, P., *Anal. Chem.* 2000, *72*, 1934–1940.

[148] Palmer, J., Burgi, D. S., Munro, N. J., Landers, J. P., *Anal. Chem.* 2001, *73*, 725–731.

[149] El-Awady, M., Huhn, C., Pyell, U., *J. Chromatogr. A* 2012, *1264*, 124–136.

[150] El-Awady, M., Pyell, U., *J. Chromatogr. A* 2013, *1297*, 213–225.

[151] Modir-Rousta, A., Bottaro, C. S., *Electrophoresis* 2013, *34*, 2553–2560.

[152] Quirino, J. P., Aranas, A. T., *Electrophoresis* 2012, *33*, 2167–2175.

[153] Zhang, S., Ma, R., Yang, X., Wang, C., Wang, Z., *J. Chromatogr. B* 2012, *906*, 41–47.

[154] Dong, Y. L., Zhang, H. G., Rahman, Z. U., Zhang, H. J., Chen, X. J., Hu, J., Chen, X. G., *J. Chromatogr. A* 2012, *1265*, 176–180.

[155] Yang, X., Cheng, X., Lin, Y., Tan, Z., Xie, L., Choi, M. M. F., *J. Chromatogr. A* 2014, *1325*, 227–233.

[156] Yang, X., Zhang, S., Wang, J., Wang, C., Wang, Z., *Anal. Chim. Acta* 2014, *814*, 63–68.

[157] Quirino, J. P., Aranas, A. T., *J. Sep. Sci.* 2012, *35*, 3514–3520.

[158] Khir, N. H. M., Jaafar, J., Bakar, M. B., *Jurnal Teknologi* 2012, *57*, 99–109.

[159] Ge, S., Tang, W., Han, R., Zhu, Y., Wang, Q., He, P., Fang, Y., *J. Chromatogr. A* 2013, *1295*, 128–135.

[160] Slouka, Z., Senapati, S., Chang, H.-C., *Ann. Rev. Anal. Chem.* 2014, *7*, 317–335.

[161] Startsev, M. A., Inglis, D. W., Baker, M. S., Goldys, E. M., *Anal. Chem.* 2013, *85*, 7133–7138.

[162] Sung, K.-B., Liao, K.-P., Liu, Y.-L., Tian, W.-C., *Microfluid. Nanofluid.* 2013, *14*, 645–655.

[163] Chen, C.-L., Yang, R.-J., *Electrophoresis* 2012, *33*, 751–757.

[164] Hsu, W.-L., Inglis, D. W., Jeong, H., Dunstan, D. E., Davidson, M. R., Goldys, E. M., Harvie, D. J. E., *Langmuir* 2014, *30*, 5337–5348.

[165] Kim, M., Kim, T., *Analyst* 2013, *138*, 6007–6015.

[166] Shin, I. H., Kim, K.-J., Kim, J., Kim, H. C., Chun, H., *Lab Chip* 2014, *14*, 1811–1815.

[167] Wang, C., Ouyang, J., Ye, D.-K., Xu, J.-J., Chen, H.-Y., Xia, X.-H., *Lab Chip* 2012, *12*, 2664–2671.

[168] Song, H., Wang, Y., Garson, C., Pant, K., *Microfluid. Nanofluid.* 2014, *17*, 693–699.

[169] Kim, B., Heo, J., Kwon, H. J., Cho, S. J., Han, J., Kim, S. J., Lim, G., *ACS Nano* 2013, *7*, 740–747.

[170] Zhang, D.-W., Zhang, H.-Q., Tian, L., Wang, L., Fang, F., Liu, K., Wu, Z.-Y., *Microfluid. Nanofluid.* 2013, *14*, 69–76.

[171] Ko, S. H., Song, Y., Kim, S. J., Kim, M., Han, J., Kang, K. H., *Lab. Chip.* 2012, *12*, 4472–4482.

[172] Kim, M., Jia, M., Kim, T., *Analyst* 2013, *138*, 1370–1378.

[173] Jeon, H., Lee, H., Kang, K. H., Lim, G., *Sci. Rep.* 2013, *3*, 3483.

[174] DongWon, C., Sang Hui, K., Hyungwan, S., Seungmin, K., YooChan, K., HyunGwang, S., Sang-Myung, L., Jeong Hoon, L., *Appl. Phys. Express* 2013, *6*, 017001.

[175] Lee, H. S., Chu, W. K., Zhang, K., Huang, X., *Lab Chip* 2013, *13*, 3389–3397.

[176] Wang, J.-Y., Xu, Z., Li, Y.-K., Liu, C., Liu, J.-S., Chen, L., Du, L.-Q., Wang, L.-D., *App. Phys. Lett.* 2013, *103*, 043103.

[177] Han, D., Kim, K. B., Kim, Y., Kim, S., Kim, H. C., Lee, J., Kim, J., Chung, T. D., *Electrochim. Acta* 2013, *110*, 164–171.

[178] Heo, J., Kwon, H. J., Jeon, H., Kim, B., Kim, S. J., Lim, G., *Nanoscale* 2014, *6*, 9681–9688.

[179] Quist, J., Trietsch, S. J., Vulto, P., Hankemeier, T., *Lab Chip* 2013, *13*, 4810–4815.

[180] Shallan, A. I., Gaudry, A. J., Guijt, R. M., Breadmore, M. C., *Chem. Commun.* 2013, *49*, 2816–2818.

[181] Chiang, P.-J., Kuo, C.-C., Zamay, T. N., Zamay, A. S., Jen, C.-P., *Microelectron. Eng.* 2014, *115*, 39–45.

[182] Wu, Z.-Y., Fang, F., He, Y.-Q., Li, T.-T., Li, J.-J., Tian, L., *Anal. Chem.* 2012, *84*, 7085–7091.

[183] Wu, J.-K., Wu, Y.-S., Yang, C.-S., Tseng, F.-G., *Biosens. Bioelec.* 2013, *43*, 453–460.

[184] Louër, A.-C., Plecis, A., Pallandre, A., Galas, J.-C., Estevez-Torres, A., Haghiri-Gosnet, A.-M., *Anal. Chem.* 2013, *85*, 7948–7956.

[185] Wang, C., Ouyang, J., Wng, Y., Ye, D., Xia, X., *Anal. Chem.* 2014, *86*, 3216.

[186] Tak, Y. H., Toraño, J. S., Somsen, G. W., de Jong, G. J., *J. Chromatogr. A* 2012, *1267*, 138–143.

[187] Maijó, I., Fontanals, N., Borrull, F., Neusüß, C., Calull, M., Aguilar, C., *Electrophoresis* 2013, *34*, 374–382.

[188] Jooß, K., Sommer, J., Bunz, S. C., Neusüß, C., *Electrophoresis* 2014, *35*, 1236–1243.

[189] Medina-Casanellas, S., Domínguez-Vega, E., Benavente, F., Sanz-Nebot, V., Somsen, G. W., de Jong, G. J., *J. Chromatogr. A* 2014, *1328*, 1–6.

[190] Wu, Y., Zhang, W., Chen, Z., *Electrophoresis* 2012, *33*, 2911–2919.

[191] Zhai, H., Li, J., Chen, Z., Su, Z., Liu, Z., Yu, X., *Microchem. J.* 2014, *114*, 223–228.

[192] Nge, P. N., Pagaduan, J. V., Yu, M., Woolley, A. T., *J. Chromatogr. A* 2012, *1261*, 129–135.

[193] Zhang, X., Xu, S., Lee, Y. I., Soper, S. A., *Analyst* 2013, *138*, 2821–2824.

[194] Phillips, T. M., Wellner, E., *Electrophoresis* 2013, *34*, 1530–1538.

[195] Mai, T. D., Bomastyk, B., Duong, H. A., Pham, H. V., Hauser, P. C., *Anal. Chim. Acta* 2012, *727*, 1–7.

[196] Polo-Luque, M. L., Simonet, B. M., Valcárcel, M., *Electrophoresis* 2013, *34*, 304–308.

[197] Liu, H., Dasgupta, P. K., *Anal. Chem.* 1996, *68*, 1817–1821.

[198] Jeannot, M. A., Cantwell, F. F., *Anal. Chem.* 1996, *68*, 2236–2240.

[199] Psillakis, E., Kalogerakis, N., *Trends Anal. Chem.* 2003, *22*, 565–574.

[200] Jain, A., Verma, K. K., *Anal. Chim. Acta* 2011, *706*, 37–65.

[201] Alothman, Z. A., Dawod, M., Kim, J., Chung, D. S., *Anal. Chim. Acta* 2012, *739*, 14–24.

[202] Cheng, K., Choi, K., Kim, J., Sung, I. H., Chung, D. S., *Microchem. J.* 2013, *106*, 220–225.

[203] Park, S. T., Kim, J., Choi, K., Lee, H. R., Chung, D. S., *Electrophoresis* 2012, *33*, 2961–2968.

[204] Kubáň, P., Boček, P., *Anal. Chim. Acta* 2013, *787*, 10–23.

[205] Pantůčková, P., Kubáň, P., Boček, P., *Electrophoresis* 2013, *34*, 289–296.

[206] Pantůčková, P., Kubáň, P., Boček, P., *J. Chromatogr. A* 2013, *1299*, 33–39.

[207] Lindenburg, P. W., Tjaden, U. R., van der Greef, J., Hankemeier, T., *Electrophoresis* 2012, *33*, 2987–2995.

[208] Payán, M. D. R., Li, B., Petersen, N. J., Jensen, H., Hansen, S. H., Pedersen-Bjergaard, S., *Anal. Chim. Acta* 2013, *785*, 60–66.

[209] Schmidt-Marzinkowski, J., See, H. H., Hauser, P. C., *Electroanalysis* 2013, *25*, 1879–1886.

[210] See, H. H., Stratz, S., Hauser, P. C., *J. Chromatogr. A* 2013, *1300*, 79–84.

[211] Kubáň, P., Boček, P., *J. Chromatogr. A* 2014, *1337*, 32–39.

[212] Furmaniak, P., Kubalczyk, P., Głowacki, R., *J. Chromatogr. B* 2014, *961*, 36–41.

[213] Wang, C. C., Lu, C. C., Chen, Y. L., Cheng, H. L., Wu, S. M., *J. Agric. Food. Chem.* 2013, *61*, 5914–5920.

[214] Anres, P., Delaunay, N., Vial, J., Thormann, W., Gareil, P., *Electrophoresis* 2013, *34*, 353–362.

[215] Tian, J., Qiao, J., Gao, J., Qin, W., *J. Chromatogr. A* 2013, *1280*, 112–116.

[216] Hernández-Mesa, M., Airado-Rodríguez, D., Cruces-Blanco, C., García-Campaña, A. M., *J. Chromatogr. A* 2014, *1341*, 65–72.

[217] Lin, E. P., Lin, K. C., Chang, C. W., Hsieh, M. M., *Talanta* 2013, *114*, 297–303.

[218] Hsu, S. H., Hu, C. C., Chiu, T. C., *Anal. Bioanal. Chem.* 2013, 1–7.

[219] Kukusamude, C., Srijaranai, S., Quirino, J. P., *Anal. Chem.* 2014, *86*, 3159–3166.

[220] Rabanes, H. R., Aranas, A. T., Benbow, N. L., Quirino, J. P., *J. Chromatogr. A* 2012, *1267*, 74–79.

[221] Tubaon, R. M., Haddad, P. R., Quirino, J. P., *J. Chromatogr. A* 2014, *1349*, 129–134.

[222] Kukusamude, C., Srijaranai, S., Kato, M., Quirino, J. P., *J. Chromatogr. A* 2014, *1351*, 110–114.

[223] Dawod, M., Chung, D. S., *J. Sep. Sci.* 2011, *34*, 2790–2799.

[224] Xu, Z., Kawahito, K., Ye, X., Timerbaev, A. R., Hirokawa, T., *Electrophoresis* 2011, *32*, 1195–1200.

[225] Xu, Z. Q., Koshimidzu, E., Hirokawa, T., *Electrophoresis* 2009, *30*, 3534–3539.

[226] Xu, Z. Q., Nakamura, K., Timerbaev, A. R., Hirokawa, T., *Anal. Chem.* 2011, *83*, 398–401.

[227] Hirokawa, T., Koshimidzu, E., Xu, Z. Q., *Electrophoresis* 2008, *29*, 3786–3793.

[228] Ye, X., Mori, S., Yamada, M., Inoue, J., Xu, Z., Hirokawa, T., *Electrophoresis* 2013, *34*, 583–589.

[229] Ye, X., Mori, S., Xu, Z., Hayakawa, S., Hirokawa, T., *Electrophoresis* 2013, *34*, 3155–3162.

[230] Song, L., Maestre, M. F., *J. Biomol. Struct. Dyn.* 1991, *9*, 525–536.

[231] Breadmore, M. C., *Electrophoresis* 2008, *29*, 1082–1091.

[232] Breadmore, M. C., *J. Chromatogr. A* 2010, *1217*, 3900–3906.

[233] Breadmore, M. C., Quirino, J. P., *Anal. Chem.* 2008, *80*, 6373–6381.

[234] Dawod, M., Breadmore, M. C., Guijt, R. M., Haddad, P. R., *J. Chromatogr. A* 2009, *1216*, 3380–3386.

[235] Meighan, M. M., Dawod, M., Guijt, R. M., Hayes, M. A., Breadmore, M. C., *J. Chromatogr. A* 2011, *1218*, 6750–6755.

[236] Giddings, J. C., *Anal. Chem.* 1984, *56*, 1258A-1270A.

[237] Česla, P., Fischer, J., Jandera, P., *Electrophoresis* 2012, *33*, 2464–2473.

[238] Wang, S., Njoroge, S. K., Battle, K., Zhang, C., Hollins, B. C., Soper, S. A., Feng, J., *Lab Chip* 2012, *12*, 3362–3369.

[239] Henley, W. H., Ramsey, J. M., *Electrophoresis* 2012, *33*, 2718–2724.

[240] Mellors, J. S., Black, W. A., Chambers, A. G., Starkey, J. A., Lacher, N. A., Ramsey, J. M., *Anal. Chem.* 2013, *85*, 4100–4106.

[241] Álvarez Porebski, P., Lynen, F., *J. Chromatogr. A* 2014, *1336*, 87–93.

[242] Horciciak, M., Masar, M., Bodor, R., Danc, L., Bel, P., *J. Sep. Sci.* 2012, *35*, 674–680.

[243] Marak, J., Stanova, A., Vavakova, V., Hrenakova, M., Kaniansky, D., *J. Chromatogr. A* 2012, *1267*, 252–258.

[244] Ginterova, P., Marak, J., Stanova, A., Maier, V., Sevcik, J., Kaniansky, D., *J. Chromatogr. B* 2012, *904*, 135–139.

[245] Mikus, P., Marakova, K., Veizerova, L., Piestansky, J., Galba, J., *J. Chromatogr. Sci.* 2012, *50*, 849–854.

[246] Mikus, P., Veizerova, L., Piestansky, J., Marakova, K., Havranek, E., *Electrophoresis* 2013, *34*, 1223–1231.

[247] Mikus, P., Koval, M., Marakova, K., Piest'ansky, J., Havranek, E., *Talanta* 2013, *103*, 294–300.

[248] Wu, R., Wang, Z., Zhao, W., Yeung, W. S., Fung, Y. S., *J. Chromatogr. A* 2013, *1304*, 220–226.

[249] Wu, R., Wang, Z., Fung, Y. S., Peng Seah, D. Y., Yeung, W. S.-B., *Electrophoresis* 2014, *35*, 1728–1734.

[250] Schure, M. R., *Anal. Chem.* 1999, *71*, 1645–1657.

6 Addendum

[2]Faculty of Science, Department of Chemistry, Universiti Teknologi Malaysia, Johor, Malaysia
[3]Faculty of Pharmacy, Department of Pharmaceutical Chemistry, Mahidol University, Rajathevee, Bangkok, Thailand
[4]Faculty of Health Sciences, School of Pharmacy, Australian Centre of Research on Separation Science, University of Tasmania, Hobart, Tasmania, Australia
[5]Ibnu Sina Institute for Fundamental Science Studies, Universiti Teknologi Malaysia, Johor, Malaysia
[6]Department of Chemistry, University of Michigan, Ann Arbor, MI, USA
[7]Faculty of Pharmacy, Department of Analytical Chemistry, Al-Azhar University, Cairo, Egypt

